2021

Allicin stimulates the phosphorylation of eNOSSer1177 via a PI3K-dependent mechanism in type-I diabetic donor coronary artery endothelial cells

Hunter Alberto Vásquez
Philadelphia College of Osteopathic Medicine

Philadelphia College of Osteopathic Medicine

Graduate Program in Biomedical Sciences

Department of Bio-Medical Sciences

Allicin stimulates the phosphorylation of eNOS^{Ser1177} via a PI3K-dependent mechanism in type-I diabetic donor coronary artery endothelial cells

A Thesis in Biomedical Sciences by Hunter Alberto Vásquez

Submitted in Partial Fulfillment of the Requirements for the Degree of Masters in Biomedical Sciences

June 2021

This thesis has been presented to and accepted by the Associate Dean for Curriculum and Research Office of Philadelphia College of Osteopathic Medicine in partial fulfillment of the requirements for the degree of Master of Science in Biomedical Sciences.
We, the undersigned, duly appointed committee have read and examined this manuscript and certify it is adequate in scope and quality as a thesis for this master's degree. We approve the content of the thesis to be submitted for processing and acceptance.

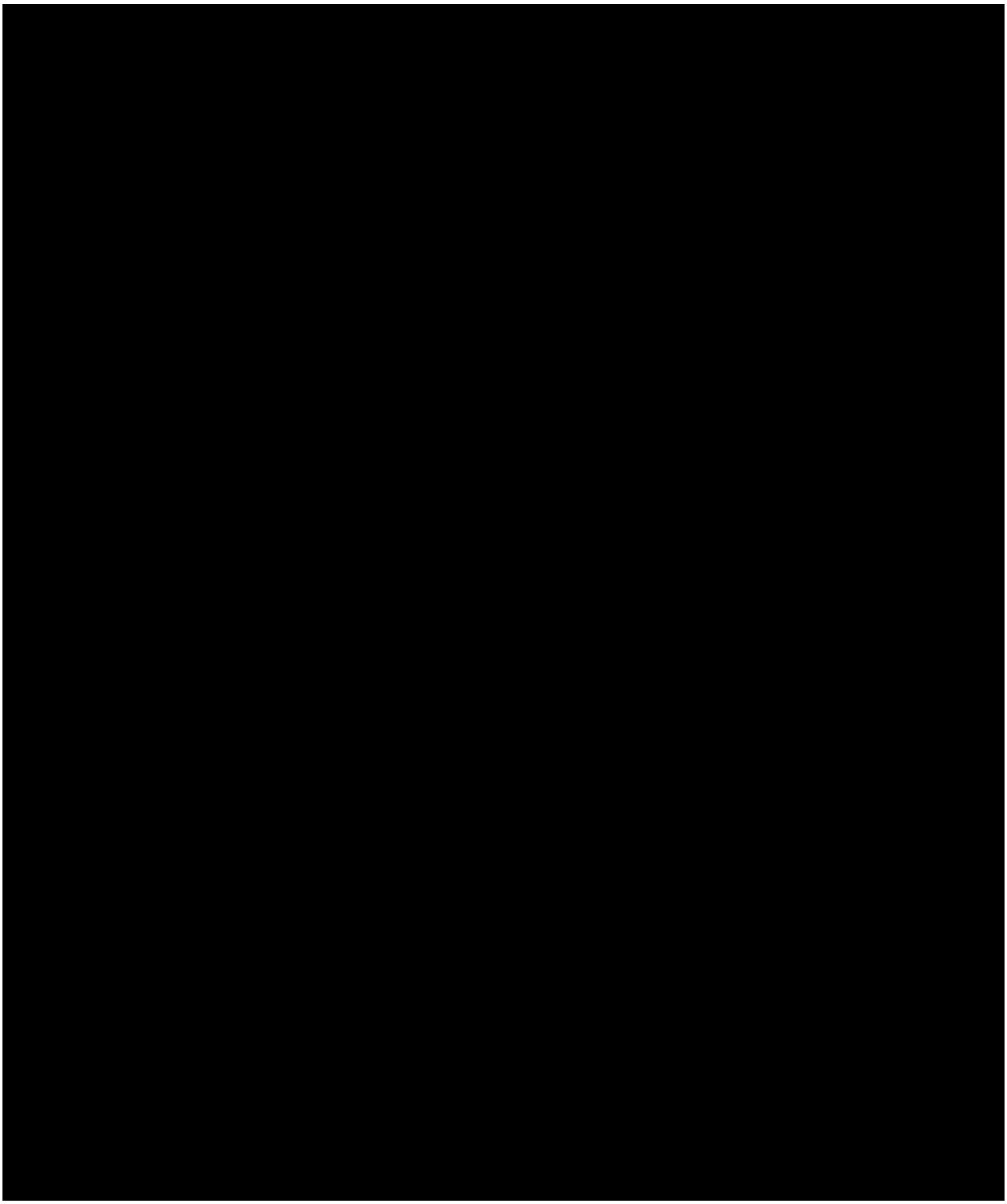

ABSTRACT

INTRODUCTION: The World Health Organization (WHO) indicates that deaths from non-communicable diseases (NCDs) are projected to increase to approximately 52 million by the year 2030. Of these NCDs, cardiovascular diseases (CVDs) constitute the number one cause of death globally and are the major source of morbidity and mortality associated with diabetes mellitus (DM). CVD manifests early in individuals with DM by way of vascular dysfunction, characterized by depressed nitric oxide (NO) production. As such, interventions to mediate the comorbidities associated with DM are being investigated.

OBJECTIVES: The primary objective of this study was to investigate the mechanism of action for allicin, a naturally-occurring compound in dietary garlic, to increase nitric oxide (NO) production in type-I diabetic donor coronary artery endothelial cells (DHCAEC-I).

METHODS: Endogenous H_2S production following healthy donor coronary artery endothelial cell (HCAEC) and DHCAEC-I treatment with allicin was measured by way of fluorescence microscopy using the cell-trappable fluorogenic probe SF7-AM. Similarly, DAF-FM DA was used to measure NO production in the presence of allicin with and without wortmannin, an inhibitor targeting PI3K. To confirm the findings of DAF-FM DA fluorescence microscopy, immunoblots targeting p-eNOS^{Ser1177}, eNOS, p-Akt^{Ser473}, and Akt were employed.

RESULTS: Treatment of HCAEC and DHCAEC-I with allicin resulted in increases in H_2S by 126% and 85%, respectively ($p < 0.01$). NO production following allicin treatment increased in DHCAEC-I by 66% ($p < 0.0001$), the effect of which was diminished by the use of wortmannin ($p < 0.0001$). eNOS^{Ser1177} phosphorylation in DHCAEC-I increased 89% from baseline after treatment with allicin ($p < 0.05$), the effect of which was also reversed by the use of wortmannin ($p < 0.01$). Allicin had no statistically-significant effects on NO production or eNOS^{Ser1177} phosphorylation in HCAEC, and had no statistically-significant effects on Akt^{Ser473} phosphorylation in HCAEC or DHCAEC-I.

CONCLUSION: These data strongly support the hypothesis that allicin-mediated NO production is dependent on PI3K in DHCAEC-I. Future experiments are needed to determine the specific involvement of H_2S and the targeted proteins downstream of PI3K.

TABLE OF CONTENTS

LIST OF FIGURES

LIST OF TABLES

ACKNOWLEDGEMENTS

Throughout the construction of this thesis, I have received a great deal of support and assistance.

First and foremost, I would first like to thank my mentor, Dr. Richard White, whose expertise and guidance has been an invaluable part of my thesis. Likewise, I would like to thank my research committee members, Drs. Shu Zhu and Harold Komiskey – your insight and feedback constantly pushed me to sharpen my critical thinking and have elevated my work as a graduate student.

I would like to sincerely thank Drs. Lori Redmond and Francis Jenney. Our weekly meetings have allowed me to think critically beyond the scope of my research and have given me insight into the biomedical implications of my research. I truly thank you for your stimulating discussions.

Lastly, I would like to thank my parents and my partner for their constant support. I truly could not have completed my work in the Biomedical Science program without your help.

INTRODUCTION

1.1 Cardiovascular Disease

The World Health Organization (WHO) indicates that deaths from noncommunicable diseases (NCDs) are projected to increase to approximately 52 million by the year 2030 (Chestnov, 2014). Of these NCDs, cardiovascular diseases (CVDs) constitute the number one cause of death globally and represent a host of heart and vascular diseases, including coronary artery disease (CAD, i.e., heart attack), cerebrovascular disease (i.e., stroke), and diseases of the aorta and arteries such as hypertension, among others (Mendis et al., 2014). CVDs are generally caused by risk factors that are divided into two categories: modifiable and non-modifiable. Of those in the latter, the most common are age, gender, and family history (Balakumar et al., 2016). Hypertension, tobacco use, physical inactivity, unhealthy diet, and diabetes mellitus (DM) constitute the most common of the risk factors that are categorized as modifiable (Balakumar et al., 2016).

1.1.1 Coronary Artery Disease

The hallmark of CAD is the impediment of blood flow through the vessel lumen of the coronary arteries resulting from the development of atherosclerotic plaques (APs) (Shahjehan and Bhutta, 2021). APs generally develop from an initial vascular insult to the tunica intima followed by recruitment of circulating monocytes (Shahjehan and Bhutta, 2021), which attach and migrate through interendothelial junctions in the tunica intima via interactions with PECAM (CD31) junctional adhesion molecules (Scott, 2004) where they become macrophages in the

subendothelial space. Any one or more of three events may then trigger the formation of foam cells from the subendothelial macrophages: 1) uptake of oxidized low-density lipoprotein (ox-LDL) through expression of scavenger receptors CD36 and SR-A (Scott, 2004); 2) excessive cholesterol esterification; and/or 3) impaired cholesterol release (Yu et al., 2013). While these subendothelial accumulations of cholesterol-laden foam cells (or "fatty streaks") are not necessarily clinically-significant, they serve as precursors for more advanced lesions characterized by a necrotic core surrounded by smooth muscle and extracellular matrix (Lusis, 2000) that may become calcified over time (Shahjehan and Bhutta, 2021). Consequently, such lesions are common risk factors for ruptures that may lead to partial or total occlusion of the coronary lumen, thus resulting in acute coronary syndromes (Shahjehan and Bhutta, 2021).

This occlusion of the coronary artery lumen, leading to the cessation of blood flow, typically results in acute myocardial infarction (MI), particularly if the cessation ranges in time between 20 and 40 minutes (Ojha and Dahmoon, 2020). In cases of coronary occlusion, what follows is lack of oxygenation of the myocardium, resulting in disruption of the sarcolemma and myofibril relaxation (Ojha and Dhamoon, 2020). With sustained cessation follows necrosis of the myocardium from the sub-endocardium to the sub-epicardium, and depending on the extent to which the necrosis has spread, could compromise normal cardiac function (Ojha and Dhamoon, 2020). Such necrotic myocardial tissue is ultimately replaced by collagenous tissue that, in quite the majority of cases, interferes with the mechanical properties of healthy myocardial tissue, such as increasing the resistance of circumferential stretch (Holmes et al., 1997), further compounding the risk factors of CVD.

1.1.2 Hypertension

Of the most notable risk factors for the morbidity and mortality associated with CVD is systemic arterial hypertension (SAH) (Oparil et al., 2018), which can be defined as persistently elevated arterial blood pressure (BP), typically exceeding systolic values of 130 mmHg and diastolic values of 80 mmHg (Iqbal and Jamal, 2020). While the pathophysiology of SAH is complex and at times multifactorial, genetic predisposition with the addition of environmental factors increases the probability SAH development (Oparil et al., 2018).

Of these environmental factors, sodium (Na^+) plays a crucial role, particularly due to its involvement in blood volume regulation. Increases in dietary Na^+ in normotensive individuals is typically followed by water retention and/or hemodynamic changes as compensatory mechanisms to maintain stable BP levels (Oparil et al., 2018); however, in addition to high water retention, sustained increases in Na^+ intake may result in increased systemic peripheral resistance, endothelial dysfunction, and changes to the structure of the large arteries (Grillo et al., 2019). For example, high Na^+ intake stimulates the retention of water through an osmolarity gradient, resulting in an increase in blood volume, which consequently increases cardiac output (CO) (Blaustein et al., 2012). As a result of the increased CO and its contribution to tissue overperfusion, total peripheral resistance (TPR) increases, thus sustaining the elevated BP (Blaustein et al., 2012).

While increased Na^+ intake is certainly a risk factor for SAH, it should be noted that the *intake* of Na^+ is not the sole contributor. In fact, dysfunctions or inappropriate activation of the renin-angiotensin-aldosterone system (RAAS) is key as well, which is a significant regulator of blood volume and vascular resistance on a prolonged basis (Fountain and Lappin, 2020). Under normal conditions, prorenin is both released by and cleaved by juxtaglomerular (JC) cells to form renin in response to decreased renal blood pressure, decreased sodium loads in the distal convoluted tubule (DCT), or beta-activation (Fountain and Lappin, 2020). Following cleavage, renin can act on the liver-produced angiotensinogen, cleaving it to angiotensin I (ATI). Lastly, the inactive ATI can be converted to the active angiotensin II (ATII) by angiotensin converting enzyme (ACE) in the vascular endothelium of the lungs and kidneys (Fountain and Lappin, 2020). ATII can subsequently bind AT receptors I and II in the kidney, adrenal cortex, arterioles, and brain, and while the full scope of AT receptor functions are still being investigated, studies have shown increases in nitric oxide (NO) production as a result (Fountain and Lappin, 2020). In addition, ATII is responsible for increasing Na^+ reabsorption directly through the Na-H exchanger in the proximal convoluted tubule (PCT), or the insertion of luminal Na^+ channels and basolateral Na^+/K^+ ATPase proteins in the DCT by way of aldosterone stimulation in the adrenal cortex (Fountain and Lappin, 2020). In all, these mechanisms are targeted to increasing Na^+ reabsorption.

While these mechanisms are well-suited for managing blood volume on a prolonged basis, inappropriate activation of the RAAS can lead to the development of hypertension (Fountain and Lappin, 2020). For example, JC cells are prone to sense a decreased blood volume subsequent to a

renal artery stenosis, and thereby activate the RAAS, resulting in increased blood volume circulation (Fountain and Lappin, 2020).

1.2 Diabetes Mellitus

DM is a disease in which the β cells of the pancreas are unable to sufficiently produce insulin due to autoimmune dysfunction (type I, T1DM) or when cellular responses to insulin are resistant (type II, T2DM) (Inzucchi et al., 2010). DM continues to be a growing epidemic in the United States with a current prevalence of more than 10% of the population (CDC, 2020) and projections that such will rise an additional 200 million by the year 2040 (Goyal and Ishwarlal, 2020). Of the myriad of secondary complications, vascular dysfunction has been observed in a large subset of these patients in a condition that has been termed diabetic vascular disease (DVD).

1.2.1 Insulin

Insulin is an anabolic peptide hormone produced by the β cells of the islets of Langerhans in the pancreas. Structurally, insulin is a single-chain polypeptide consisting of both proinsulin and a signal peptide, the former being released after translocation into the endoplasmic reticulum (Vargas et al., 2021). After release, proinsulin's A and B chains, which are joined continuously through a C domain, are cleaved to release insulin (A and B chains linked via a disulfide bond) independently along with C-peptide (Vargas et al., 2021).

The soluble insulin peptide hormone exerts its effects through binding of insulin receptors (INSRs) on target cells such as those in skeletal muscle, adipose tissue, and the liver (Petersen and Shulman, 2018). INSRs comprise an $\alpha_2\beta_2$ heterotetramer consisting of two α-subunits and two β-subunits, the former of which are extracellular and the latter being transcellular and containing cytoplasmic tyrosine kinase domains (Hubbard et al., 2013). While there are two isoforms of INSRs, A and B, the B isoform is more metabolically relevant in adults with a high specificity in the skeletal muscle, adipose tissue, and particularly in hepatic cells (Petersen and Shulman, 2018).

Functionally, insulin stimulates the uptake of glucose via transmembrane glucose transporter (GLUT) proteins, predominantly via GLUT4 in the skeletal muscle and adipose tissue and GLUT2 in the liver (Vargas et al., 2020). Insulin-mediated glucose uptake regulated by GLUT4, for example, follows that insulin begins by binding to the α-subunit of an INSR, stimulating the phosphorylation of one β subunit on specific tyrosine residues within INSR's activation loop as well as autophosphorylation of other tyrosine residues within the intracellular tail (Chang et al., 2004). This INSR activation subsequently mediates the phosphorylation of insulin receptor substrates (IRS) 1-4 (Chang et al., 2004), which bind and activate phosphatidylinositol 3-kinase (PI3K), in turn activating Akt (note: the PI3K/Akt pathway is described in detail in section 1.5). Upon activation of Akt, intracellular GLUT4-rich vesicles translocate to the cell membrane, inserting GLUT4 transcellularly and facilitating the uptake of glucose (Wang et al., 2020).

1.2.2 Type I Diabetes Mellitus

T1DM is a chronic autoimmune disease resulting in the destruction of the β-cells in the pancreatic islets, subsequently resulting in the secondary decrease in the production of insulin (Lucier and Weinstock, 2021), an anabolic peptide hormone responsible for the regulation of glucose uptake in the peripheral tissues and metabolism of carbohydrates, lipids, and proteins (Wilcox, 2005). While the precise etiology of T1DM is multifaceted, and much remains elusive, the disease is a well-studied heritable polygenic disease with approximately 50% of the prevalence being linked to two human leukocyte antigen (HLA) major histocompatibility complex II (MHC class II) haplotypes: HLA-DR3-DQ2 and HLA-DR4-Q8 (DiMeglio et al. 2018). While diagnosis of T1DM through HLA risk or familial risk have increased, non-HLA loci have been associated with risk for T1DM as well, yielding early diagnoses problematic, as non-HLA loci alone cannot be used to predict the development of T1DM (DiMeglio et al. 2018).

While genetic predispositions account for approximately half of the cases of T1DM (DiMeglio et al. 2018), a number of environmental factors may also play an important role in the pathogenesis. Originally described by epidemiological observations, exposure to viruses (i.e., rubella or enteroviruses) or toxins and nutrients (cow's milk and cereals) may contribute to the generation of pancreatic autoantibodies, though the specific effects of these factors remain unclear (Paschou et al., 2017).

The onset of T1DM typically begins in stage 1 of 3, characterized by normal fasting glucose and glucose tolerance, with ≥2 pancreatic autoantibodies (Lucier and Weinstock, 2021). The progression to stage 2 is marked by ≥2 pancreatic autoantibodies with the addition of dysglycemia (impaired fasting glucose or glucose tolerance, or hemoglobin A1c between 5.7-6.4%), followed by stage 3 being characterized by hyperglycemia (Lucier and Weinstock, 2021).

1.2.3 Type II Diabetes Mellitus

While T1DM is a cell-mediated autoimmune dysfunction of pancreatic β-cells, T2DM is associated with β-cell dysfunction (Goyal and Ishwarlal, 2020), insulin resistance in the peripheral tissues (Freeman and Pennings, 2020), or both, and accounts for the majority of all cases of DM (Goyal and Ishwarlal, 2020). Of the peripheral tissues, the three primary sites of insulin resistance are the muscle tissue, adipose tissue, and the liver (Freeman and Pennings, 2020), typically beginning in the muscle (Zhang et al., 2019) as it accounts for 70% of glucose uptake (Freeman and Pennings, 2020), thus having a large effect on the turnover of glucose (DeFronzo and Tripathy, 2009).

The mechanisms of action for insulin resistance in skeletal muscle are complex, however a number of studies, first being suggested by Randle et al. (1963), have proposed an association between INSR sensitivity and saturated fatty acids. This study in particular, termed the “Randle Cycle”, proposes that increased fatty acid (β) oxidation increases the production of acetyl CoA, increasing both the levels of citrate and the ratio of ATP/ADP, and consequently the inhibition of

phosphofructokinase (PFK), accumulation of glucose 6-phosphate, and inhibition of hexokinase, finally resulting in increased intracellular glucose and thus reduced glucose uptake (Martins et al., 2012). An interesting and contrasting consideration, however, finds that intracellular glucose accumulation must not necessarily precede its uptake inhibition. Later studies conducted by Roden et al. (1996) have suggested that glucose uptake is inhibited by increased plasma fatty acids. These studies were further reinforced by the findings that INSRs are inhibited by the activation of a number of kinases including protein kinase C (PKC), inhibitor of nuclear factor kappa β (IKKβ), c-Jun N-terminal kinase (JNK), and p38 mitogen-activated protein (MAP) kinase, through phosphorylation-mediated proteosome degradation (Martins et al., 2012).

Modern studies have described muscle insulin resistance induced via lipids including diacylglycerols (DAGs), triacylglycerols (TAGs), and ceramides. Szebdridei et al. (2014) and Yu and Pekkurnaz (2018) have demonstrated a marked increase in DAGs and PKCθ signaling, which subsequently impairs IRS-1 activation via tyrosine phosphorylation (Martins et al., 2012). As such, the IRS-1/PI3K/Akt signaling cascade is diminished, preventing insulin-stimulated glucose uptake via GLUT proteins (Martins et al., 2012).

As obesity is a well-recognized risk factor for T2DM, an important consideration to its development is both the amount and distribution of adipose tissue, which has autocrine, paracrine, and endocrine functions in the secretion of various adipokines such as leptin, adiponectin, resistin, tumor necrosis factor-α (TNF-α), and interleukin-6 (IL-6) (Pittas et al., 2004). These adipokines can further be designated as insulin sensitizers and insulin antagonists.

Of the insulin sensitizers, both leptin and adiponectin maintain an essential role in energy homeostasis. Studies on leptin deficient (*ob*/*ob*) mice reveal conditions including obesity and T2DM, the effect of which is reversed via the administration of leptin (Zhang et a., 1994). Leptin has also been postulated to increase insulin sensitivity in peripheral tissues including the skeletal muscle and liver (Unger et al., 1999 and Minokoshi et al., 2002). Similarly, adiponectin has been shown to have a negative correlation with obesity (Arita et al., 1999), diabetic dyslipidemia (Matsubara et al., 2002), and particularly with insulin resistance (Weyer et al., 2001). In another model, administration of adiponectin to lipoatrophic mice reverses obesity and syndromes associated with T2DM (Yamauchi et al., 2001).

The actions of insulin antagonists may also, at least to an extent, mediate T2DM. Resistin, for example, has been shown to impair glucose tolerance and insulin action when administered in normal mice, and while data still remain to be fully illustrated, suggests that resistin may impair the actions of insulin on hepatic glucose production (Rajala et al., 2003). Similarly, mRNA of the proinflammatory cytokine TNF-α has been shown to correlate positively with conditions including hyperinsulinemia (Kern et al., 1995), possibly in part by facilitating increased free fatty acid release by adipocytes and decreased adiponectin synthesis (Bruun et al., 2003). Lastly, IL-6, another proinflammatory cytokine, is also partly responsible for decreasing insulin sensitivity by mechanisms similar to TNF-α (Boden and Shulman, 2002 and Fasshauer et al., 2003) in mouse models that developed obesity and glucose intolerance (Wallenius et al., 2002); however,

evidence is conflicting in healthy human models who remained glucose-tolerant (Steensberg et al., 2003).

While the exact mechanism has not been fully elucidated, hepatic insulin resistance is a major contributor to systemic insulin resistance (Zhang et al., 2020), and insulin resistance in the skeletal muscle and adipose tissue as previously described may stem from hepatic insulin resistance (Badi et al., 2019). Hepatic insulin resistance follows a similar mechanism involving DAGs, TAGs, and ceramides that accumulate in hepatic cells and stimulate PKC-ε, which in turn downregulates insulin receptor kinase and IRS-1 and -2 tyrosine phosphorylation (Zhang et al., 2020) as previously described. Hepatic insulin resistance and T2DM have been demonstrated to be almost ubiquitous sequelae in individuals with non-alcoholic fatty liver disease (NAFLD), for example, with greater than 90% of obese patients with NAFLD presenting with T2DM (Perry et al., 2014). Given that hepatic DAG content along with other lipids are such strong predictors for NAFLD with subsequent hepatic insulin resistance, regulation of fat delivery to the liver has been a chief focus of biomedical research. Interestingly, Doege and colleagues (2008) have found that knockdown of the primary fatty acid transporter in hepatocytes, fatty acid transporter protein 5, via RNA interference demonstrated a marked reduction in fatty acid uptake in mice that improved whole-body glucose homeostasis and reversed NAFLD, reinforcing the contribution of lipids in the development of hepatic insulin resistance and T2DM.

1.2.4 Diabetes-Induced Vascular Dysfunction

The negative effects of glucose begin to occur at thresholds below hyperglycemic levels in a concept known as the "glycemic continuum", exacerbated by insulin resistance or impairment and culminating in structural and functional endothelial (vascular) dysfunction: the impaired production of endothelium-derived vasodilating and -constricting factors (Paneni et al., 2013 and Daiber et al., 2017). Factors that mediate dilation include endothelium-derived relaxing factor (EDRF), endothelium-derived hyperpolarizing factor (EDHF), prostacyclin, and of particular interest, nitric oxide (NO), while the primary vasoconstricting factor is endothelin-I (Daiber et al., 2017). One such causal link between hyperglycemia and decreased NO production is the generation of reactive oxygen species (ROS) induced by hyperglycemia, contributing to polyol flux, generation of advanced glycosylation end products (AGEs), PKC activation, and activation of nuclear factor kappa light-chain enhancer of B cells (NF-κB) (Paneni et al., 2013). A prominent contributor to ROS generation involves the aforementioned activation of PKC, stemming from the elevation of DAG in a hyperglycemic endothelial environment and leading to an increase in nicotinamide adenine dinucleotide phosphate (NADPH) oxidase-induced superoxide production (Paneni et al., 2013). Indeed, ROS generation is a key contributor to endothelial dysfunction, however, the bioavailability of NO, in particular, is affected as well via the downregulation of endothelial nitric oxide synthase (eNOS) activity (Paneni et al., 2013), limiting the dilatory capacity of the endothelium. It should be noted that ROS can also facilitate endothelial dysfunction by directly scavenging NO or by eNOS uncoupling through the oxidative phosphorylation of tetrahydrobiopterin (Funk et al., 2012). Further contributing to the generation of ROS in hyperglycemic conditions is the retention of non-insulin-dependent GLUTs, in contrast to insulin-dependent GLUTs, that are downregulated in these conditions. Non-insulin-

dependent GLUTs allow for the constitutive uptake of extracellular glucose for enhanced glycolytic oxidation and subsequent electron shuttling, stimulating oxidative stress and downstream eNOS uncoupling (Funk et al., 2012).

Another prominent contribution to endothelial dysfunction involves the generation of hyperglycemia-induced AGEs, the nonenzymatic addition of aldose carbohydrates to proteins in a process termed the Milliard reaction (Funk et al., 2012). In this reaction, Schiff bases are formed via the addition of a reducing sugar such as glucose or fructose to the α-amino group of the N-terminus of a protein or to lysine, followed by rearrangement to form ketoamines and subsequently AGEs via either oxidative or nonoxidative pathways (Funk et al., 2012). While these products tend to have little clinical significance in healthy humans, hyperglycemia causes excessive glycation of proteins found both in the serum (i.e., albumin) and in the vessel wall (i.e., collagen) (Funk et al., 2012). The formation of these modified proteins has deleterious effects on eNOS coupling both directly and indirectly. In the former, AGEs facilitate the decrease in eNOS expression and L-citrulline production while inhibiting histamine-induced NO production in the latter (Funk et al., 2012).

1.3 Vascular Endothelium and Coronary Artery Anatomy

The common structure of a blood vessel comprises three layers: the tunica intima, tunica media, and tunica adventitia (externa), which are composed of a single layer of endothelial cells, vascular smooth muscle (VSM), and elastic lamina, respectively, from innermost to outermost

(Dhananjayan et al., 2016). At its most basic level, the endothelium serves as a selectively permeable barrier, regulating the transport of macromolecules between the lumen and VSM layer, largely being restricted by interendothelial junctions at the endothelial cells' lateral borders (Cahill and Redmond, 2016). The endothelium is also largely responsible for the maintenance of homeostatic functions via a precise balance between regulatory vasoactive factors such as NO, endothelin-I, angiotensin and other adhesion molecules and cytokines (Dhananjayan et al., 2016). Via these mechanisms, the endothelium tightly regulates blood flow, delivery of nutrients, and inflammation (Dhananjayan et al., 2016). As such, these endogenous factors are implicated in vascular responses that impact blood flow at a local level.

This thesis will focus exclusively on human endothelial cells of the coronary arteries and their roles in vasodilation. The coronary arteries arise from the aorta within the left and right cusps of the aortic valve to give rise to both the left main and right coronary arteries (LMCA and RCA), respectively (Villa et al., 2016). The LMCA primarily supplies the left atrium and ventricle and divides into two branches: the left anterior descending branch and the circumflex artery (Ogobuiro et al., 2020). The RCA supplies the right atrium and ventricle, as well as the sinoatrial and atrioventricular nodes, and divides into the right posterior descending branch and the acute marginal artery (John's Hopkins, 2020). Because there is a linear relationship between blood flow and myocardial oxygen consumption (Saxton et al., 2020), and because of the endothelial regulatory functions on vascular tone, it is important to understand the relationship between dilatory substances such as NO and their role in the diseased state, such as in DM.

1.4 Nitric Oxide Synthase

While the VSM response to sympathetic stimulation largely contributes to vascular tone, namely throughout the vascular tree (Cahill and Redmond, 2016), vascular tone and blood flow are both highly regulated by NO, which is enzymatically formed by nitric oxide synthase (NOS) at a local level (Chen et al., 2008). As such, the bioavailability of NO is totally dependent on NOS. To date, there are three isoforms of NOS that have been elucidated: neuronal NOS (nNOS, NOS1), inducible NOS (iNOS, NOS2), and eNOS (NOS3) (Chen et al., 2008). The latter represents a pathway by which there are numerous stimuli for activation, including shear stress, vascular endothelial growth factor (VEGF), estradiol, sphingosine 1-phosphate, and bradykinin, among others, that act in calcium-dependent and -independent pathways (Sessa, 2014). In the former, these stimuli can activate phospholipase C-γ, causing an increase in cytoplasmic calcium and DAG concentrations (Sessa, 2014). The increased calcium subsequently activates calmodulin (CaM), which binds to the CaM-binding domain on eNOS and stimulates the synthesis of NO (Sessa, 2014). A number of these stimuli may also activate the PI3K/Akt pathway, one that is calcium-independent and tightly controlled via a multistep process (Sessa, 2014).

1.5 PI3K/Akt/eNOS Pathway

PI3K is a heterodimeric protein containing a regulatory subunit and catalytic subunit known as p85 and p110, respectively (Cantrell, 2001), and is involved in a wide-range of cellular processes including protein synthesis, trafficking, regulation of enzyme activity, and proliferation, among others (Ciraolo et al., 2014). The activation of PI3K begins with binding of receptor tyrosine kinases (RTKs), which can be facilitated by a number of stimuli, including hormones, growth

factors, and components of the extracellular matrix (Nicholson et al., 2002), as well as through transactivation via the Gα subunit of G-protein coupled receptors (GPCRs) (New et al., 2011). Upon binding of these substances to the extracellular N-terminal domain or through activation via Gα, RTKs undergo dimerization and autophosphorylation of the tyrosine residues in the intracellular domain (Shi et al., 2019). Subsequently, PI3K is recruited to the membrane by the p85 subunit, the Src homology 2 (SH2) domain of which binds the pYXXM motif of the tyrosine-phosphorylated RTK (Jiang et al., 2014), followed by recruitment of the p110 subunit (Liu et al., 2009). It should be noted that there are three other pathways that can activate PI3K as well: in the first, the pYXXM-bound growth factor receptor-bound protein 2 (GRB2) binds GRB2-associated binding protein (GAB), which in turn binds the p85 subunit of PI3K (Castellano and Downward, 2011) followed by recruitment of p110. In the second, the pYXXM-bound GRB2 binds the guanine nucleotide exchange factor Son of Sevenless (SOS), which in turn binds and activates RAS, and finally activates the p110 subunit of PI3K without the need for p85 (Castellano and Downward, 2011). Lastly, the p110 subunit of PI3K can be directly activated by the Gβγ subunit of GPCRs (New et al., 2011).

The activation of PI3K subsequently yields phosphorylation of phosphatidylinositol 4,5-bisphosphate (PIP2) forming phosphatidylinositol 3,4,5-triphosphate (PIP3), and provides docking sites for proteins such as Akt (Liu et al., 2009). Because of its high affinity for PIP3 (Miao et al., 2010), the pleckstrin homology (PH) domain of Akt translocates to PIP3 on the membrane and induces conformational changes on Akt that exposes residues Thr^{308} and Ser^{473}. It is important to note that full activation of Akt requires phosphorylation of both of these residues,

Thr^{308} being phosphorylated by phosphoinositide-dependent kinase 1 (PDK1) (Dangelmaier et al., 2014), and Ser^{473} phosphorylated by phosphoinositide-dependent kinase 2 (PDK2), integrin-linked kinase (ILK) (Osaki et al., 2004), mechanistic target of rapamycin complex (mTORC) (Sarbassov et al., 2005), and DNA-dependent protein kinase (DNA-PK) (Feng et al., 2004).

Upon full activation of Akt, the downstream effector, eNOS, can be phosphorylated at a number of residues, thereby increasing or decreasing eNOS activity, and thus have opposing effects. For example, the Thr^{495} domain acts as an inhibitory site while Ser^{635} and Ser^{1177} act as activation sites (Zhao et al., 2015). Activation of eNOS through Ser^{635} or Ser^{1177} subsequently yields catalysis of the five-electron oxidation of a guanidine nitrogen on L-arginine, yielding NO and L-citrulline as a byproduct (Barbato and Tzeng, 2004) in the presence of molecular oxygen and NADPH (Chen et al., 2008). (Figure 1).

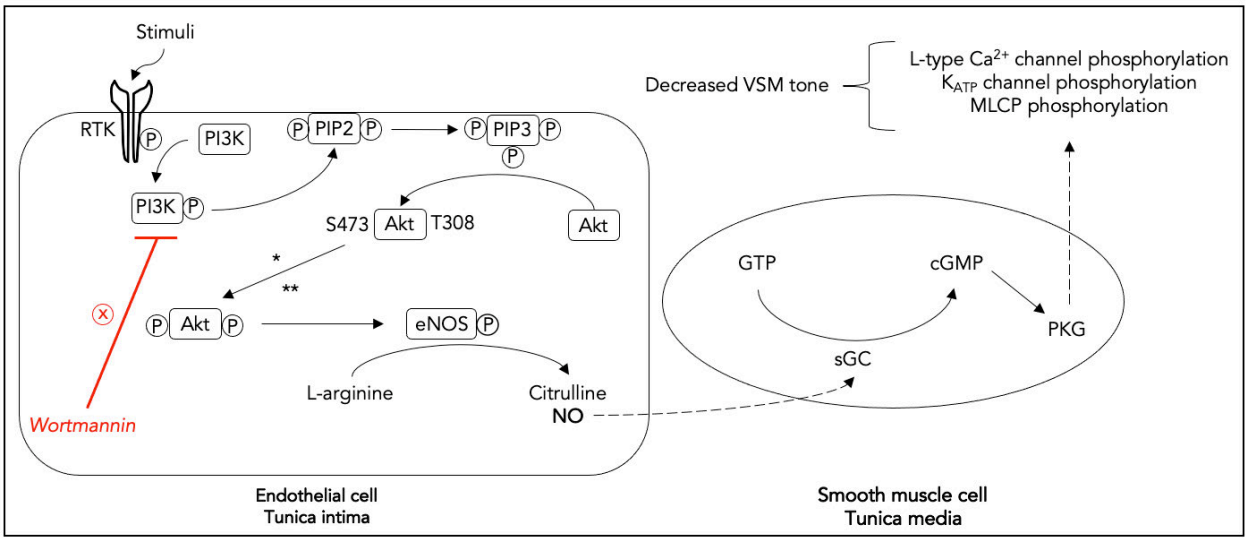

Figure 1. ***Schematic of the PI3K/Akt/eNOS pathway and NO-mediated vasodilation.*** ** = PDK2, ILK, mTORC, DNA-PK; ** = PDK1.*

1.6 Nitric Oxide-Mediated Vasodilation

Upon diffusion from the endothelium to the VSM, NO binds an N-terminal heme moiety of its heterodimeric primary receptor, soluble guanylate cyclase (sGC) (Montfort et al., 2017). This binding forms a penta-coordinated iron-NO complex (Pan et al., 2017) and subsequently converts guanosine triphosphate (GTP) to a second messenger, guanosine 3,5-cyclic monophosphate (cGMP), initiating the cGMP signaling pathway (Pasmanter et al., 2020) and resulting in protein kinase G (PKG) activation (Francis et al., 2010).

PKG ultimately induces VSM relaxation through three individual mechanisms: 1) phosphorylation of L-type calcium channels, thus reducing calcium influx and preventing contraction (Takimoto and Kass, 2012); 2) phosphorylation of ATP-sensitive potassium channels resulting in hyperpolarization (Han et al., 2002); and 3) phosphorylation of myosin light chain phosphatase (MLCP), which in turn dephosphorylates myosin light chain kinase (MLCK), thus preventing the cross-bridge action of actin and myosin, yielding vasorelaxation (Landry et al., 2006) (Figure 1).

1.7 Allicin and Garlic-Derived Sulfides

Alliin is an inactive sulfoxide that is derived from the hydrolysis or oxidation of γ-glutamylcysteine found in raw, dietary garlic (*Allium sativum*) (Amagase et al., 2001). Upon

ingestion, there is activation of the garlic-derived allinase enzyme, which converts the inactive alliin into its active form called diallyl thiosulfinate (or allicin) (Amagase et al., 2001). This unstable active compound readily breaks down into three organic polysulfides: diallyl sulfide (DAS), diallyl disulfide (DADS), and diallyl trisulfide (DATS) (Banerjee and Maulik, 2002). Furthermore, previous research indicates that these polysulfides produce hydrogen sulfide (H_2S) via thiol-dependent cellular and glutathione (GSH)-dependent acellular reactions (Benadives et al., 2007). While H_2S is well-known to be a toxic gas that is produced endogenously via L-cysteine (Hosoki et al., 1997), Predmore et al. (2011) have demonstrated that H_2S upregulates NO production via an Akt-dependent mechanism in bovine arterial endothelial cells (BAECs).

1.8 Preliminary Data

Horuzsko et al. (2019) have demonstrated that treatment of healthy human donor coronary artery endothelial cells (HCAEC), type-I diabetic human donor coronary artery endothelial cells (DHCAEC-I), and type-II diabetic human donor coronary artery endothelial cells (DHCAEC-II) with allicin increases NO production in DHCAEC-I but not in HCAEC nor DHCAEC-II. As measured by EVOS imaging, allicin increased mean fluorescence intensity in DHCAEC-I by >292% compared to untreated cells, indicating an increase in NO production. Further, immunoblot analysis revealed that there was no statistically-significant difference in untreated vs. treated HCAEC or DHCAEC-II eNOS expression; however, eNOS expression in DHCAEC-I increased by approximately 26% when treated with 5 μM allicin overnight. Given that NO production follows the required phosphorylation at a positively-regulating motif on eNOS, these data suggest that allicin mediates the restoration of NO and is eNOS-dependent.

1.9 Proposed Pathway

Previous literature has supported that garlic-derived polysulfides induce H_2S production via a thiol-dependent manner. The unstable active allicin readily breaks down into DAS, DADS, and DATS *in vivo* and *in vitro* and act as H_2S donors when reacting with biological thiols such as GSH (Benavides et al., 2007). Further, treatment of BAECs with H_2S has demonstrated a time-dependent 87% increase in NO production at 30 minutes post-treatment, and because it is not elevated at subsequent times, this suggests a transient activation of eNOS (Predmore et al., 2011), which may possibly be attributed to changes in the enzyme's phosphorylation status. Data strongly suggest that the phosphorylation of eNOS surrounding the Ser^{1177} motif ($RIRTQS^{1177}F$) is a result of upstream activation of Akt, which is a downstream target of PI3K (Michell et al., 1999). In BAECs treated with H_2S, the Akt inhibitor triciribine prevented an increase in $eNOS^{Ser1177}$ phosphorylation, suggesting that H_2S stimulates eNOS phosphorylation via an Akt-dependent mechanism (Predmore et al., 2011). Further, attenuation of PI3K with the inhibitor wortmannin has demonstrated a decrease in the phosphorylation of PI3K, Akt, and eNOS (Song et al., 2016), lending support to the pathway proposed herein.

In summary, it is proposed that allicin-derived polysulfides stimulate the PI3K/Akt pathway and result in downstream phosphorylation of eNOS at the Ser^{1177} motif, this pathway being responsible for increased NO production in DHCAEC-I.

METHODS

2.1 Cell Culture

Passage (P) 2 HCAEC (Lonza) and DHCAEC-I (Lonza) from a 21-year-old (y.o) male donor and a 29 y.o female donor, respectively, were removed from liquid nitrogen in sterile cryovials combined with dimethyl sulfoxide (DMSO) and grown in 5 mL endothelial cell basal growth media (EBM-2, Lonza) and supplemented with microvascular endothelial SingleQuots kit (Lonza) and 1% penicillin/streptomycin at 37 °C and 5% CO_2 until a confluence of ≥90% was reached. Both cell types were subsequently passaged via the addition of 0.25% trypsin/EDTA (1X, Thermo Fischer) and incubated at 37 °C for 3 minutes to facilitate cell detachment. Once the cells were fully detached, fresh EBM-2 was added, and cells were divided between 3 flasks and re-incubated. To maintain an optimal growth environment, cell media was exchanged every two days.

2.2 Hydrogen Sulfide Production

2.2.1 Mechanism of SF7-AM

Sulfidefluor-7 acetoxymethyl ester (SF7-AM, Cayman Chemical) is a membrane-permeable, non-fluorescent indicator of H_2S production. Upon entry into the cell, the acetoxymethyl ester groups are hydrolyzed by intracellular esterases, yielding a negatively-charged SF7, rendering the compound membrane-impermeable and thus remaining trapped inside the cell (Lin et al., 2013). Once trapped inside the cell, SF7 is weakly-fluorescent; however, in the presence of H_2S, the azide functional groups are reduced to primary amines, forming a highly-fluorescent

derivative (SF7-D) (Lin et al., 2013), allowing for relative quantifications of H_2S at nanomolar concentrations. (Figure 2).

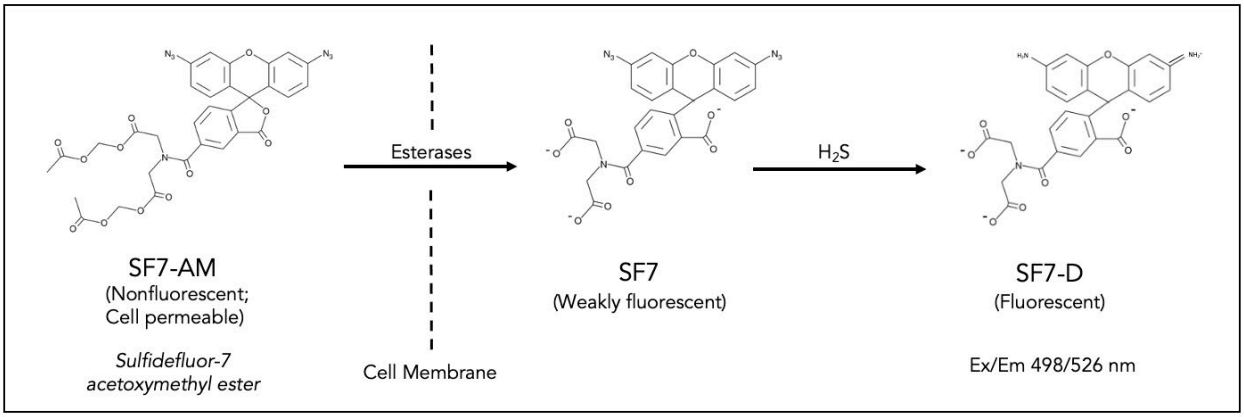

Figure 2. ***Schematic of the mechanism for SF7-AM.***

2.2.2 Baseline Hydrogen Sulfide Imaging

Aliquots of 1.5 mL P4 HCAEC and DHCAEC-I were plated separately in groups of three until a confluence of 60% was reached, with the following conditions: 1) untreated; 2) treated with 5 µM allicin (Table 1). 24 hours prior to imaging, the EBM-2 was aspirated and replaced with 1.5 mL phenol red free EBM-2 (PRFM, Lonza). 500 µL 2.5 µM SF7-AM/PRFM was added to the cells under a dark hood and incubated in the dark at 37 °C and 5% CO_2 for 30 minutes followed by aspiration and washing three times with 1 mL PRFM. For baseline imaging, cells were incubated for 30 minutes once more with 500 µL PRFM and imaged using an EVOS microscope at 40X with a GFP filter (ex/em 498/526 nm).

HCAEC		DHCAEC-I	
Untreated	+ 5 μM allicin	Untreated	+ 5 μM allicin

Table 1. Experimental design and treatment allocation for the measurement of H_2S.

2.2.3 Allicin Treatment Hydrogen Sulfide Imaging

After baseline imaging, cells were washed three times with 1 mL PRFM. After the last wash, cells were treated with 500 μL 5 μM allicin (Santa Cruz Biotechnology)/PRFM and incubated in the dark at 37 °C and 5 % CO_2 for 20 minutes. Images were captured at 40X with a GFP filter (ex/em 498/526 nm). The calculation for allicin dilution is shown below:

$$\frac{10\ mg\ allicin}{mL} * \frac{1\ g}{1000\ mg} * \frac{1000\ mL}{1\ L} * \frac{1\ mol}{162.27\ g\ allicin} = \frac{10{,}000}{162{,}270} = 0.0616256\ M$$

$$= 61.6256\ mM\ allicin$$

$$1{:}\,10\ dilution = 10\ \mu L\ allicin + 90\ \mu L\ ddH_2O = 6.16256\ mM\ allicin\ stock$$

$$V_1 = \frac{C_2V_2}{C_1} = \frac{(0.005\ mM\ final\ concentration)(2\ mL\ final\ volume)}{6.16256\ mM\ allicin\ stock}$$

$$= 0.0016227\ mL\ allicin\ stock = 1.6227\ \mu L\ allicin\ stock\ in\ 2\ mL\ PRFM = 5\ \mu M\ allicin$$

2.3 Nitric Oxide Production

2.3.1 Mechanism of DAF-FM DA

4-amino-5-methylamino-2', 7'-difluorofluorescein diacetate (DAF-FM DA, Thermo Fischer) is a membrane-permeable, non-fluorescent indicator of NO production. Upon entry into the cell, the

acetate groups are hydrolyzed by intracellular esterases, yielding a negatively-charged DAF-FM, rendering the compound membrane-impermeable and thus remaining trapped inside the cell (Cortese-Krott et al., 2012). Once trapped inside the cell, DAF-FM is weakly-fluorescent; however, in the presence of NO and oxygen ($NO\bullet + O_2 \rightarrow N_2O_3$), a highly-fluorescent benzotriazole derivative (DAF-BT D) is formed (Cortese-Krott et al., 2012), allowing for relative quantifications of NO at nanomolar concentrations (Ghebremariam et al., 2013) (Figure 3).

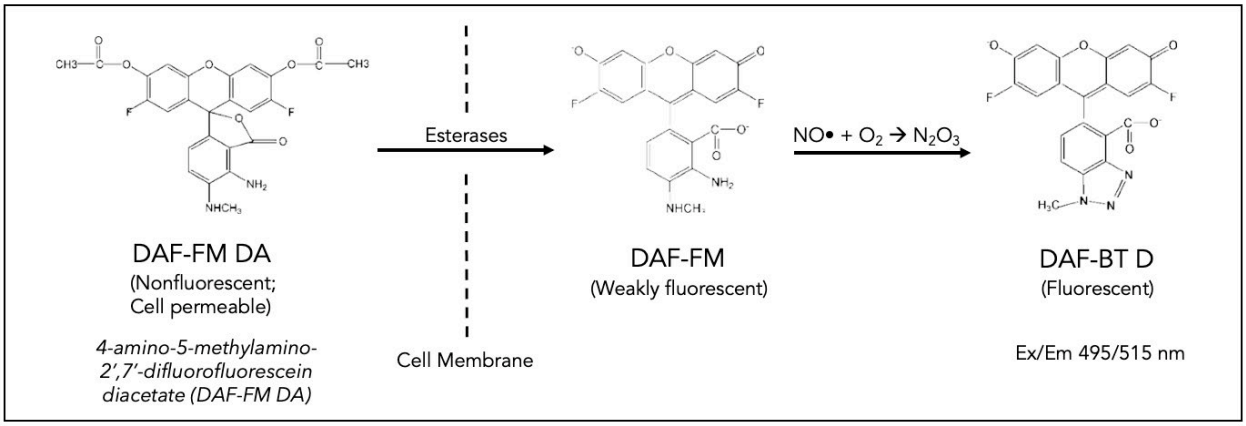

Figure 3. ***Schematic of the mechanism for DAF-FM DA.***

2.3.2 Baseline Nitric Oxide Imaging

Aliquots of 1.5 mL P4 HCAEC and DHCAEC-I were plated separately in groups of three until a confluence of 60% was reached, with the following conditions: 1) untreated; 2) treated with 5 µM allicin; 3) pretreated with 5 µM wortmannin (an inhibitor of PI3K; Sigma Aldrich) followed by treatment with 5 µM allicin (Table 2). 24 hours prior to imaging, the EBM-2 was aspirated and replaced with 1.5 mL PRFM. 500 µL 10 µM DAF FM-DA/PRFM was added to the cells under a dark hood and incubated in the dark at 37 °C and 5% CO_2 for 30 minutes followed by aspiration

and washing three times with 1 mL PRFM. For baseline imaging, cells were incubated for 30 minutes once more with 500 µL PRFM and imaged using an EVOS microscope at 40X with a GFP filter (ex/em 495/515 nm).

HCAEC			**DHCAEC-I**		
Untreated	+ 5 µM allicin	+ 5 µM WRT + 5 µM allicin	Untreated	+ 5 µM allicin	+ 5 µM WRT + 5 µM allicin

Table 2. Experimental design and treatment allocation for the measurement of NO. WRT = wortmannin.

2.3.3 Allicin Treatment Nitric Oxide Imaging

After baseline imaging, cells were washed three times with 1 mL PRFM. After the last wash, cells were treated with 500 µL 5 µM allicin/PRFM and incubated in the dark at 37 °C and 5 % CO_2 for 20 minutes. Images were captured at 40X with a GFP filter (ex/em 495/515 nm).

2.3.4 Wortmannin Pretreatment Nitric Oxide Imaging

To measure the effects of PI3K inhibition, cells were incubated with 500 µL 10 µM DAF-FM DA/PRFM for 30 minutes at 37 °C and 5 % CO_2, followed by aspiration and washing three times with 1 mL PRFM. Subsequently, cells were incubated with 500 µL 5 µM wortmannin for 30 minutes, aspirated and washed three times with 1 mL PRFM, and incubated for 20 minutes with 500 µL 5 µM allicin at 37 °C and 5 % CO_2. Cells were imaged using an EVOS microscope at 40X with a GFP filter (ex/em 495/515 nm).

2.4 Phospho-eNOS and Phospho-Akt Immunoblots

P4 HCAEC and DHCAEC-I were grown in sets of three separate 100 mm cell culture dishes to ≥90% confluence in 10 mL EBM-2. Prior to protein collection, one dish of each set remained untreated with 10 mL PRFM only, one received 10 mL 5 μM allicin/PRFM, and one was pretreated with 10 mL 5 μM wortmannin for 30 minutes followed by addition of 8.113 μL allicin (final concentration = 5 μM) (Table 3). The three culture dishes of each cell type were subsequently incubated for 20 minutes at 37 °C and 5% CO_2 followed by washing with 25 mL 1X phosphate buffered saline (PBS).

Cells were lysed with 100 μL ice cold 1X radioimmunoprecipitation assay (RIPA) lysis buffer (Thermo Fischer) for 1 hour on ice and centrifuged at 21,754 g for 10 minutes. Cell supernatants were transferred to new Eppendorf tubes and protein concentrations were determined with a Pierce bicinchoninic acid kit (Thermo Fischer). Samples were prepared by combining 70 μg of protein with 10 μL 4X Laemmli Sample Buffer (Bio-Rad) and 1X PBS to a total volume of 40 μL, followed by boiling at approximately 95 °C for 5 minutes. 40 μL of the samples were loaded in Mini-PROTEAN TGX 4-20% 10-well precast gels (Bio-Rad). Sodium dodecyl sulfide polyacrylamide gel electrophoresis (SDS-PAGE) of both treated and untreated HCAEC and DHCAEC-I were carried out in triplicate with 1X Tris/Glycine/SDS buffer (Bio-Rad) for approximately 2 hours at 100 V followed by transfer to a polyvinylidene difluoride (PVDF) membrane using a Bio-Rad Trans-Blot Turbo Transfer System in 1X Trans-Blot Turbo Transfer Buffer (Bio-Rad). PVDF membranes were then rinsed with and washed in 1X PBS with 1% Tween20 (Fischer BioReagents, PBST) for 5 minutes while shaking at room temperature,

followed by incubation with Odyssey Blocking Buffer in PBS (Li-Cor) for 1 hour while shaking at room temperature.

Primary antibodies against phospho-eNOS^{Ser1177} (rabbit, monoclonal, Invitrogen, 1:1000 dilution), eNOS (mouse, monoclonal, BD Biosciences, 1:700 dilution), phospho-Akt^{Ser473} (mouse, monoclonal, Proteintech, 1:1000 dilution), Akt (mouse, monoclonal, Proteintech, 1:2000 dilution), and β-actin (mouse, monoclonal, Li-Cor, 1:5000 dilution) were diluted in 5 mL Odyssey Blocking Buffer with 10% Tween20 and incubated with the PVDF membranes overnight while shaking at 4 °C. On the following day, the membranes were incubated for one additional hour while shaking at room temperature and subsequently washed three times with PBST: once for 15 minutes and twice more for 5 minutes. After washing, the membranes were incubated with a goat anti-rabbit or goat anti-mouse antibody (monoclonal, Li-Cor, 1:5000 dilution) solution in 5 mL Odyssey Blocking Buffer, 10% SDS, and 10% Tween20 for 1 hour while shaking at room temperature. Following incubation with secondary antibody, membranes were washed three times with PBST: once for 15 minutes and twice more for 5 minutes, and PBS twice for 5 minutes. Membranes were visualized using a Li-Cor Odyssey CLx Imaging System.

HCAEC			**DHCAEC-I**		
Untreated	+ 5 μM allicin	+ 5 μM WRT + 5 μM allicin	Untreated	+ 5 μM allicin	+ 5 μM WRT + 5 μM allicin

Table 3. ***Experimental design and treatment allocation for the measurement of p-eNOS^{Ser1177} and p-Akt^{Ser473}.*** WRT = wortmannin.

2.5 Statistical Analysis

All experiments were conducted on three separate days with three separate cultures for statistical purposes and data are expressed as means ± SD. Pixel intensity for all EVOS data and immunoblot data were assessed using ImageJ software. H_2S data were analyzed via paired t-test; NO data, phospho-eNOS^{Ser1177} immunoblot data, and phospho-Akt^{Ser473} immunoblot data were analyzed via one-way ANOVA with Tukey's post-hoc; total eNOS expression comparisons were analyzed via two-sample t-test. Graphs were generated using GraphPad Prism software.

RESULTS

3.1 Allicin stimulates H_2S production in HCAEC and DHCAEC-I

Allicin stimulated H_2S production in both HCAEC and DHCAEC-I as indicated by SF7 mean fluorescence intensity (MFI). Baseline SF7 MFI in HCAEC was 27.412 ± 2.462 arbitrary units (AU; n = 3) and increased after addition of 5 µM allicin to 61.953 ± 5.712 AU ($p < 0.01$ compared to baseline; n = 3), representing a 126% increase in H_2S production. In DHCAEC-I, baseline SF7 MFI was 37.211 ± 3.557 AU (n = 3), which increased by 85% after the addition of 5 µM allicin (68.945 ± 4.248 AU; $p < 0.01$ compared to baseline; n = 3). Data are expressed as mean ± SD. Student's paired t-test was performed. (Figure 4).

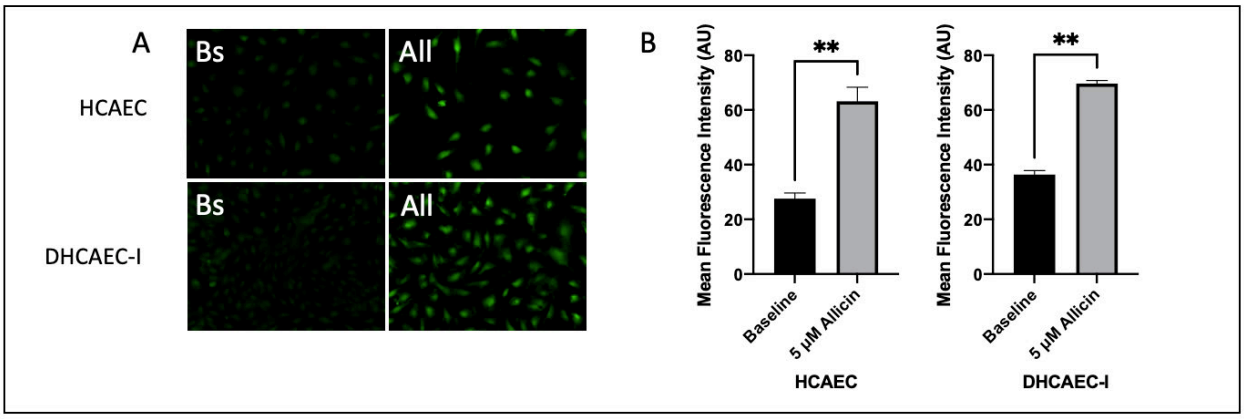

Figure 4. ***H_2S production in HCAEC and DHCAEC-I detected by SF7-AM.*** **A)** *Representative fluorescence microscopy images of HCAEC and DHCAEC-I at baseline, prior to allicin treatment (Bs) and after 20-minute treatment with 5 µM allicin (All).* ***B)*** *Quantification of relative H_2S production through mean fluorescence intensity. Results are displayed as mean ± SD. ** = $p < 0.01$.*

3.2 Allicin stimulates NO production and wortmannin reverses this effect in DHCAEC-I

Allicin stimulated NO production in DHCAEC-I and PI3K inhibition by wortmannin prevented an increase in NO production. In DHCAEC-I, baseline DAF fluorescence was 12.468 ± 0.468 AU, and 5 μM allicin treatment increased MFI by 66% (20.798 ± 0.403 AU; $p < 0.0001$ compared to baseline; $n = 3$). In cells pretreated with 5 μM wortmannin followed by allicin treatment, this effect was diminished with a MFI of 11.070 ± 0.451 AU ($p < 0.0001$ compared to allicin only; $p < 0.05$ compared to baseline; $n = 3$). (Figure 5).

In HCAEC, baseline MFI was 12.110 ± 0.105 AU ($n = 3$), and 11.718 ± 0.643 AU ($p < 0.50$ compared to baseline; $n = 3$) after treatment with 5 μM allicin. In cells pretreated with 5 μM wortmannin followed by 5 μM allicin, MFI was 10.795 ± 0.445 AU ($p < 0.05$ compared to allicin only; $p < 0.01$ compared to baseline; $n = 3$). All data are expressed as mean ± SD. One-way ANOVA with Tukey's post-hoc was performed. (Figure 5).

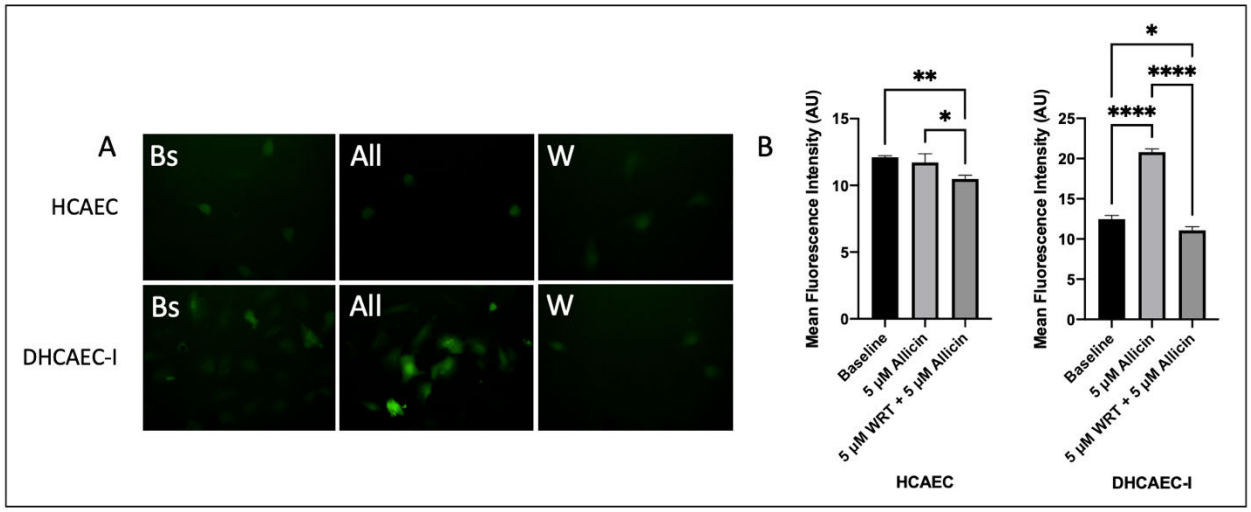

Figure 5. ***NO production in HCAEC and DHCAEC-I detected by DAF-FM DA. A)*** *Representative fluorescence microscopy images of HCAEC and DHCAEC-I at baseline, prior to allicin treatment (Bs), after 20-minute treatment with 5 µM allicin (All), and after 5 µM allicin treatment in cells pretreated with 5 µM wortmannin (W).* ***B)*** *Quantification of relative NO production through mean fluorescence intensity. Results are displayed as mean ± SD. * = $p < 0.05$, ** = $p < 0.01$, **** = $p < 0.0001$.*

3.3 Allicin increases eNOS^{Ser1177} phosphorylation and wortmannin reverses this effect in DHCAEC-I

Allicin treatment of DHCAEC-I with 5 µM allicin increased eNOS phosphorylation at Ser^{1177} from baseline (0.496 ± 0.087 AU; n = 3) to 0.938 ± 0.184 AU ($p < 0.05$ compared to baseline; n = 3), representing an 89% increase in eNOS phosphorylation. However, in DHCAEC-I pretreated with 5 µM wortmannin, the effect of allicin was diminished, returning MFI to levels similar to baseline (0.245 ± 0.113 AU; $p < 0.01$ compared to allicin only; $p < 0.13$ compared to baseline; n = 3). (Figure 6).

In HCAEC, allicin had no effect on eNOS^{Ser1177} phosphorylation (0.904 ± 0.361 AU; n = 3) compared to baseline (0.967 ± 0.235 AU; $p < 0.95$; n = 3). Similarly, in HCAEC pretreated with 5 μM wortmannin, allicin did not increase phosphorylation (0.671 ± 0.166 AU; $p < 0.56$ compared to allicin only; $p < 0.41$ compared to baseline; n = 3). All phospho-eNOS^{Ser1177} data are expressed as mean ± SD. β-actin was used as a loading control for all immunoblots. One-way ANOVA with Tukey's post-hoc was performed. (Figure 6).

Lastly, total eNOS expression was elevated in DHCAEC-I compared to HCAEC. Mean total eNOS expression (eNOS/β-actin) in HCAEC at baseline was 0.438 ± 0.005 AU (n = 3) compared to 0.803 ± 0.071 AU in DHCAEC-I ($p < 0.001$; n = 3). All total eNOS expression data are expressed as mean ± SD. Student's two-sample t-test was performed. (Figure 6).

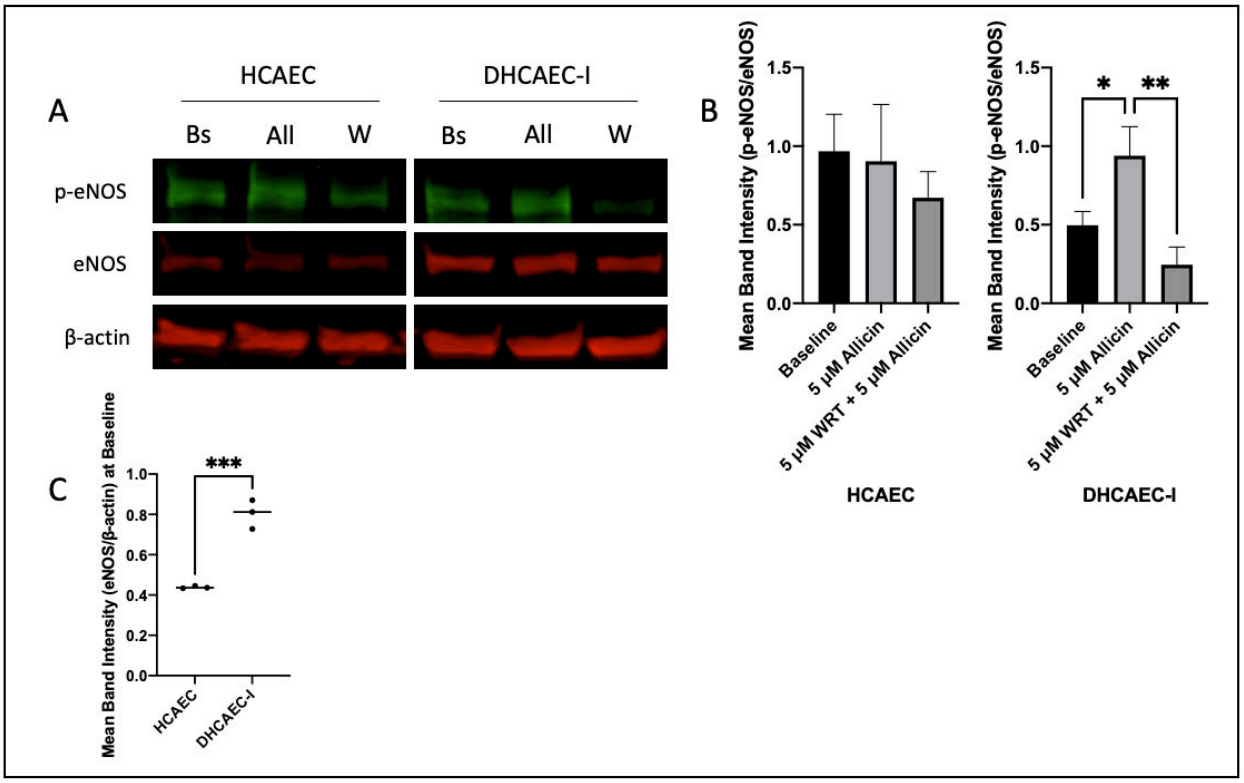

Figure 6. ***Phosphorylation of eNOS^{Ser1177} in HCAEC and DHCAEC-I. A)*** *Representative immunoblot analysis for p-eNOS^{Ser1177} and total eNOS in HCAEC and DHCAEC-I at baseline, prior to allicin treatment (Bs), after 20-minute treatment with 5 μM allicin (All), and after 5 μM allicin treatment in cells pretreated with 5 μM wortmannin (W).* ***B)*** *Quantification of eNOS^{Ser1177} phosphorylation relative to total eNOS through mean band intensity.* ***C)*** *Quantification of total eNOS expression relative to β-actin at baseline through mean band intensity. Results are displayed as mean ± SD. * = $p < 0.05$, ** = $p < 0.01$, *** = $p < 0.001$.*

3.4 Allicin has no statistically-significant effect on Akt^{Ser473} phosphorylation

5 μM allicin treatment of HCAEC decreased phosphorylation of Akt^{Ser473} from 1.618 ± 0.310 AU (n = 3) to 1.476 ± 0.396 AU ($p < 0.87$ compared to baseline; n = 3). Further, in HCAEC pretreated with 5 μM wortmannin followed by 5 μM allicin treatment, mean band intensity (MBI) was 1.436 ± 0.337 AU ($p < 0.98$ compared to allicin only; $p < 0.80$ compared to baseline; n = 3). In DHCAEC-I, 5 μM allicin treatment increased Akt^{Ser473} phosphorylation from baseline

(1.151 ± 0.323 AU) to 1.301 ± 0.324 AU ($p < 0.82$; $n = 3$); however, these data were not statistically-significant. With pretreatment of 5 μM wortmannin followed by 5 μM allicin, MBI was 1.010 ± 0.274 AU ($p < 0.51$ compared to allicin only; $p < 0.84$ compared to baseline; $n = 3$). All data are expressed as mean ± SD. β-actin was used as a loading control for all immunoblots. One-way ANOVA with Tukey's post-hoc was performed. (Figure 7).

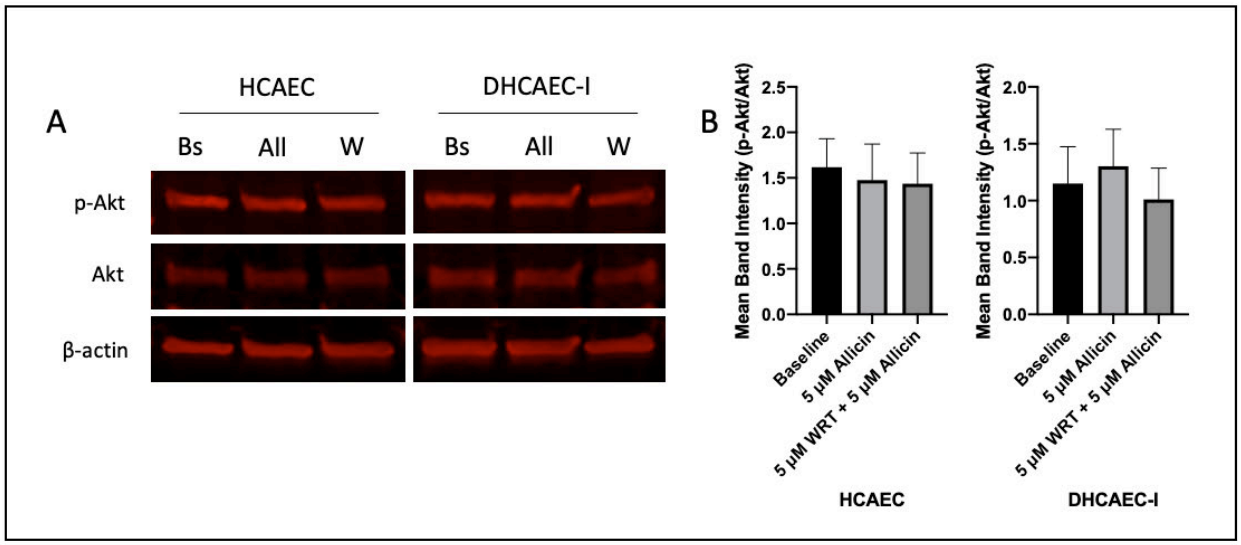

Figure 7. ***Phosphorylation of Akt^{Ser473} in HCAEC and DHCAEC-I.*** ***A)*** *Representative immunoblot analysis for p-Akt^{Ser473} in HCAEC and DHCAEC-I at baseline, prior to allicin treatment (Bs), after 20-minute treatment with 5 μM allicin (All), and after 5 μM allicin treatment in cells pretreated with 5 μM wortmannin (W).* ***B)*** *Quantification of Akt^{Ser473} phosphorylation relative to total Akt through mean band intensity. Results are displayed as mean ± SD.*

DISCUSSION

HCAEC play a principal role in the maintenance of endothelial/vascular health through the balance of vasodilating (NO, EDRF, EDHF, prostacyclin) and constricting factors (endothelin-I). However, insults to vascular integrity increases the risk for pro-atherogenic effects and manifestations related to the development of CVD, exacerbated by factors such as ROS and AGEs. The chief endothelium-derived factor for maintaining hemodynamic homeostasis is NO; as T1DM and T2DM increase the likelihood for the aforementioned CVDs stemming from DM-induced endothelial dysfunction, new interventions are being explored. With respect to naturally-occurring allyl thiosulfinates, allicin is the most abundant and studied member and has demonstrated lipid-lowering, antioxidant, anti-atherosclerotic, and anticancer effects (Lawson and Hunsaker, 2018). Horuzsko et al. (2019) have demonstrated that allicin alleviates endothelial dysfunction by increasing NO in DHCAEC-I; however, the mechanism of action remained to be elucidated. Here, we have demonstrated that allicin exerts its effects on $eNOS^{Ser1177}$ phosphorylation via a PI3K-dependent mechanism. Allicin significantly increased NO production ($p < 0.0001$) and $eNOS^{Ser1177}$ phosphorylation ($p < 0.05$), the effects of which were reversed by inhibiting PI3K via the use of wortmannin ($p < 0.0001$ and $p < 0.01$, respectively) in DHCAEC-I.

These data provide strong implications on the alleviation of endothelial dysfunction via increasing eNOS-dependent NO production and build on previous findings by Ma et al. (2018). Their particular study suggested that allicin attenuates apoptosis induced by ischemic or hypoxic events in H9c2 myoblasts through eNOS. It was shown that treatment of H9c2 myoblasts with

allicin significantly reversed the effects of intermittent hypoxia-induced increases in malondialdehyde and decreases in superoxide dismutase; further, these effects of allicin were diminished by the use of L-arginine methyl ester (L-NAME), an inhibitor of eNOS activity, reinforcing the involvement of eNOS in allicin-mediated cardioprotection (Ma et al., 2018). Moreover, allicin has been linked to improvements in cardiac functions by reducing cardiomyocyte size and decreasing B-type natriuretic peptide (BNP) and β-myosin heavy chain (β-MHC) (Ba et al., 2019). BNP, a hormone secreted by ventricular cardiomyocytes in response to stretch (Novack and Zevitz, 2020), and β-MHC, the major protein comprising myosin in cardiomyocytes (Krenz and Robbins, 2004), both serve as biomarkers for hypertrophic cardiomyopathy. Ba et al. (2019) have demonstrated that expression of both BNP and β-MHC from cardiomyocytes in rats with cardiac hypertrophy decreased after treatment with allicin, underscoring the hypertrophic relief provided by our compound of interest.

In our study, while NO production and phosphorylation of eNOS^{Ser1177} increased in DHCAEC-I after treatment with 5 μM allicin ($p < 0.0001$ and $p < 0.05$, respectively), it should be noted that we did not observe this effect in HCAEC. We currently propose two different hypotheses for these findings: 1) given that HCAEC are presumed to be healthy with no indications of endothelial dysfunction, it is plausible that any treatments to increase NO may not have a significant difference in cells with an optimal level of NO production and eNOS^{Ser1177} phosphorylation. For example, we see that the mean band intensity in the immunoblots targeting p-eNOS^{Ser1177} is 0.967 ± 0.275 AU in HCAEC, while that of DHCAEC-I is 0.496 ± 0.087 AU – approximately 48% less than baseline phosphorylation in HCAEC. 2) As there are varying

mechanisms to stimulate eNOS, it is possible that different cell types may use different pathways or motifs in these phosphorylation cascades. For one, eNOS phosphorylation can occur at a number of motifs that may be activating or deactivating: aside from Ser^{1177}, Ser^{1179}, Ser^{633}, and Ser^{615} all participate in positive regulation of eNOS (Rafikov et al., 2011). However, this second suggestion does not account for the fact that we did not see an increase in NO production under fluorescence microscopy.

Notably, we discovered a marked difference between baseline expressions of eNOS between HCAEC and DHCAEC-I. In DHCAEC-I, baseline total eNOS expression was approximately 83% higher compared to HCAEC. We hypothesize that this is likely due to a mechanism in DHCAEC-I to compensate for the reduced bioavailability of NO that is typically seen in DM-induced endothelial dysfunction. These suggestions stem from data collected by Takahashi and Harris (2014) in which eNOS expression was found to be increased early after the onset of diabetes and decreased with the disease's progression. Many cases of endothelial dysfunction, particularly in DM, are accompanied by an upregulation of eNOS expression, likely as a (futile) counter-regulatory mechanism that ultimately results in superoxide anion production in lieu of NO (Li et al., 2002 and Musicki and Burnett, 2007). We therefore suspect that the notable increase in total eNOS expression seen in DHCAEC-I compared to HCAEC is the result of a compensatory mechanism to increase baseline NO production.

Another very interesting finding from our research was that we did not see a significant change in Akt^{Ser473} phosphorylation as we initially expected. We hypothesized that activation of PI3K

would stimulate PIP2/PIP3 and subsequently the phosphorylation of Akt at Ser^{473} and Thr^{308}. As previously described, full activation of Akt requires the phosphorylation of both residues, and as such, we expected to observe an increase in the phosphorylation of Akt^{Ser473} given that PI3K is clearly involved in this pathway. We now suspect the possibility that Akt^{Ser473} may not be directly associated with an increase in PI3K-dependent phosphorylation after stimulation with allicin in DHCAEC-I. This suggestion stems from the work conducted by Kobayashi et al. (2009) in which internal mammary artery endothelial cells with experimental insulin resistance demonstrated that the Thr^{308} site of Akt was significantly impaired, whereas that of total Akt expression and phosphorylation at the Ser^{473} site were not affected, thus directly contradicting our initial expectations and supporting this new notion. As such, the phosphorylation of Thr^{308} by PDK1 is likely more closely tied with insulin impairment, providing a likely explanation for our data. Given this newfound information, our future studies involving this pathway will be closely targeted on measuring the phosphorylation at Akt^{Thr308} as opposed to Ser^{473}. It should also be noted that our initial proposal included the use of the triciribine, which prevents the activation, phosphorylation, and signaling of Akt, in our NO fluorescence microcopy and $eNOS^{Ser1177}$ immunoblot experiments; however, we were unable to obtain this inhibitor to confirm Akt's involvement.

One of the major potential contributors to the allicin-mediated activation of PI3K that results in downstream phosphorylation of eNOS and subsequent NO production is the generation of H_2S. As allicin is a relatively unstable compound, it readily breaks down into three organic polysulfides: DAS, DADS, and DATS, which have previously been shown to produce H_2S via

thiol-dependent cellular and glutathione (GSH)-dependent acellular reactions (Benavides et al., 2007). We have successfully demonstrated that allicin results in a significant increase in H_2S production in both HCAEC and DHCAEC-I ($p < 0.01$); however, we have not elucidated the mechanism nor role of H_2S in this pathway. Given that the vasodilatory effects of allicin were reversed in DHCAEC-I pretreated with a PI3K inhibitor, we suspect that H_2S is likely stimulating PI3K, either directly or indirectly. This assumption correlates with a number of studies, including one conducted by Lin and colleagues (2020), in which H_2S was found to alleviate hyperglycemia-induced inactivation of the PI3K/Akt/eNOS pathway in human umbilical vein endothelial cells (HUVECs). In this particular study, normoglycemic (control) HUVECs had p-PI3K/PI3K, p-Akt/Akt, and p-eNOS/eNOS ratios ranging between 0.75 to 0.85; however, exposure of these cells to hyperglycemic conditions reduced all ratios by >50%, and administration of NaHS (a H_2S donor) returned all ratios to near normoglycemic levels of phosphorylation. Moreover, these data reinforce studies conducted by Manna and Jain (2011) in which high glucose-induced decreases in PI3K and increases in phosphatase and tensin homolog (PTEN; a negative regulator of PI3K) were reversed via treatment with H_2S in adipocytes.

Given that PI3K phosphorylation can be mediated by RTKs (among other pathways), we now suspect that H_2S is directly stimulating vascular endothelial growth factor receptor subtype 2 (VEGFR2), a RTK on the endothelial cell surface. Data collected by Tao et al. (2013) demonstrated that H_2S could directly activate VEGFR2, and small interfering RNA (siRNA) knockdown of VEGFR2 prevented downstream phosphorylation of PI3K. VEGFR2 contains an intracellular disulfide bond between Cys1045-Cys1024 that serves as an inhibitory motif.

However, upon diffusion into the cell, H_2S reduces the Cys1045-Cys1024 bond (S–S → Cys–SH + HS–SH) via nucleophilic attack, diminishing the inhibitory consequences of the bond (Tao et al., 2013) and allowing for subsequent dimerization and autophosphorylation that is typical in RTKs, resulting in downstream PI3K activation. We therefore propose that allicin-derived H_2S is functioning as a "molecular switch", reducing the Cys1045-Cys1024 bond in VEGFR2 and mediating the PI3K-dependent phosphorylation of $eNOS^{Ser1177}$.

While we have indeed demonstrated that PI3K is involved in allicin-mediated phosphorylation of eNOS, it is worthy to note that allicin-derived H_2S may also target eNOS directly though S-sulfhydration, a posttranslational modification that targets cysteine residues (Altaany et al., 2014). S-nitrosylation, the covalent attachment of NO to the thiol group of cysteine residues (Qin et al., 2013), reversibly attenuates eNOS activity (Wang et al., 2019). Interestingly, Altaany et al. (2014) have found that S-sulfhydration and S-nitrosylation competitively modify eNOS at Cys^{443} and that S-sulfhydration of eNOS decreases S-nitrosylation at the same residue. While S-sulfhydration after NaHS treatment does not directly cause phosphorylation of eNOS, it does indirectly promote its phosphorylation by inhibiting the NO-induced concentration-dependent S-nitrosylation (Altaany et al., 2014).

Given its structure, and as previously described, allicin is readily unstable and ultimately breaks down into polysulfides in both aqueous and ethanoic solutions. Our allicin stock solution was supplied in a solution of methanol:water:formic acid, and subsequently diluted with double distilled water and maintained at -80 °C, and brought to room temperature for no more than 20

minutes during use. In a study conducted by Fujisawa et al. (2008), allicin demonstrated biological and chemical half-lives of 6 and 11 days, respectively; however, the duration of their study was conducted at room temperature (20-22 °C). In a separate study observing the long-term stability of garlic products, it was determined that there was no loss of any thiosulfinate between 3 and 24 months upon storage at -80 °C. While we cannot definitively conclude that there was no breakdown of our allicin during thawing periods at room temperature without the use of mass spectrometry, we are confident that our compound maintained its stability and purity throughout the duration of our research.

Lastly, given that allicin was supplied via a stock vehicle containing both methanol and formic acid, it is prudent to acknowledge potential confounds in our data. While methanol is known for systemic cytotoxicity, Oyama et al. (2002) demonstrated no statistically-significant differences in cell viability up to concentrations of 3 mM. Given that our allicin vehicle concentration was diluted from 61.6256 mM to 5 μM (a >1000X dilution), we suspect that the effects of methanol had a negligible impact on our results. While formic acid, an inhibitor of cytochrome oxidase, has been described as a hypoxia- and acidosis-inducing agent (Liesivuori, 2014), our study revealed no demonstrable data that NO production, $eNOS^{Ser1177}$ phosphorylation, or normal cell morphology was affected. These data stem from our results that allicin did not stimulate NO production nor $eNOS^{Ser1177}$ phosphorylation in HCAEC, though did stimulate both effects in DHCAEC-I. Further, both cell types maintained similar morphologies pre- and post-allicin treatment. We, therefore, suspect that neither methanol nor formic acid had any statistically-

significant confounding effects in our study, though future experiments with a vehicle control at similar concentrations are needed to confirm these assumptions.

Collectively, our data provide evidence supporting the hypothesis that allicin stimulates eNOS-dependent NO production via the stimulation of PI3K, however further *in vitro* studies are needed to fully elucidate the mechanism and *in vivo* studies to support its use in the prevention of T1DM-induced CVD. Our data illustrate that allicin increases H_2S production, NO production, and the phosphorylation of $eNOS^{Ser1177}$, and that the latter two are dependent on PI3K in DHCAEC-I. However, allicin has no apparent effect on HCAEC aside from H_2S production.

SUMMARY

Our data strongly support the hypothesis that allicin can alleviate T1DM-induced reductions and bioavailability of NO in human coronary artery endothelial cells. Our findings provide supporting evidence that allicin 1) increases H_2S production in HCAEC and DHCAEC-I; 2) increases NO production in DHCAEC-I only; and 3) increases $eNOS^{Ser1177}$ phosphorylation in DHCAEC-I only. These findings provide a preliminary understanding of the allicin's vasodilatory mechanism and a new direction in drug development for the treatment of CVD in T1DM.

REFERENCES

Abdul-Ghani, M. A., & DeFronzo, R. A. (2010). Pathogenesis of insulin resistance in skeletal muscle. *Biomed Research International, 2010*, 1-11. Retrieved from https://www.hindawi.com/journals/bmri/2010/476279/

Altaany, Z., Ju, Y., Yang, G., & Wang, R. (2014). The coordination of S-sulfhydration, S-nitrosylation, and phosphorylation of endothelial nitric oxide synthase by hydrogen sulfide. *Science Signaling, 9*(7) Retrieved from https://pubmed.ncbi.nlm.nih.gov/25205851/

Amagase, H., Petesch, B. L., Matsuura, H., Kasuga, S., & Itakura, Y. (2001). Intake of garlic and its bioactive components. *J Nutr., 131*, 955-962. Retrieved from https://pubmed.ncbi.nlm.nih.gov/11238796/

Anatomy and function of the coronary arteries. Retrieved Aug 2, 2020, from https://www.hopkinsmedicine.org/health/conditions-and-diseases/anatomy-and-function-of-the-coronary-arteries

Arita, Y., Kihara, S., Ouchi, N., Takahashi, M., Maeda, K., Miyagawa, J., et al. (1999). Paradoxical decrease of an adipose-specific protein, adiponectin, in obesity. *Biochemical and Biophysical Research Communications, 257*(1), 79-83. Retrieved from https://pubmed.ncbi.nlm.nih.gov/10092513/

Badi, R. M., Mostafa, D. G., Khaleel, E. F., & State, H. H. (2019). Resveratrol protects against hepatic insulin resistance in a rat's model of non-alcoholic fatty liver disease by down-regulation of GPAT-1 and DGAT2 expression and inhibition of PKC membranous translocation. *Clinical and Experimental Pharmacology and Physiology,* Retrieved from https://onlinelibrary.wiley.com/doi/epdf/10.1111/1440-1681.13074

Bae, L., Gao, J., Chen, Y., Qi, H., Dong, C., Pan, H., et al. (2019). Allicin attenuates pathological cardiac hypertrophy by inhibiting autophagy via activation of PI3K/akt/mTOR and MAPK/ERK/mTOR signaling pathways. *Phytomedicine, 58* Retrieved from https://www.sciencedirect.com/science/article/pii/S094471131830583X

Balakumar, P., Maung-U, K., & Jagadeesh, G. (2016). Prevalence and prevention of cardiovascular disease and diabetes mellitus. *Pharmacological Research, 113*, 600-609.

Banerjee, S. K., & Maulik, S. K. (2002). Effect of garlic on cardiovascular disorders: A review. *Nutritional Journal, 1*(4), 1-14. Retrieved from https://pubmed.ncbi.nlm.nih.gov/12537594/

Barbato, J. E., & Tzeng, E. (2004). *Nitric oxide and arterial disease*. United States: Mosby, Inc. doi:10.1016/j.jvs.2004.03.043

Blaustein, M. P., Leenen, F. H., Chen, L., Golovina, V. A., Hamlyn, J. M., Pallone, T. L., et al. (2012). How NaCl raises blood pressure: A new paradigm for the pathogenesis of salt-dependent hypertension. *American Journal of Physical Hear Circulation Physiology, 302*, 1031-1049. Retrieved from https://journals.physiology.org/doi/pdf/10.1152/ajpheart.00899.2011

Boden, G., & Shulman, G. I. (2002). Free fatty acids in obesity and type 2 diabetes: Defining their role in the development of insulin resistance and beta-cell dysfunction. *European Journal of Clinical Investigation, 32*, 14-23. Retrieved from https://pubmed.ncbi.nlm.nih.gov/12028371/

Bradley, J. M., Organ, C. L., & Lefer, D. J. (2016). Garlic-derived organic polysulfides and myocardial Protection123. *The Journal of Nutrition, 146*(2), 403S-409S. doi:10.3945/jn.114.208066

Bruun, J. M., Lihn, A. S., Verdict, C., Pedersen, S. B., Tuobro, S., Astrup, A., et al. (2003). Regulation of adiponectin by adipose tissue-derived cytokines: In vivo and in vitro investigations in humans. *American Journal of Physiology-Endodrinology and Metabolism, 285*(3), E527-E533. Retrieved from https://pubmed.ncbi.nlm.nih.gov/12736161/

Cahill, P. A., & Redmond, E. M. (2016). Vascular endothelium - gatekeeper of vessel health. *Atherosclerosis, 248*, 97-109. doi:10.1016/j.atherosclerosis.2016.03.007

Cantrell, D. A. (2001). Phosphoinositide 3-kinase signalling pathways. *Journal of Cell Science, 114*(Pt 8), 1439-1445. Retrieved from https://pubmed.ncbi.nlm.nih.gov/11282020/

Centers for Disease Control and Prevention. (2020). National diabetes statistics report: Estimates of diabetes and its burden in the united states. Retrieved from https://www.cdc.gov/diabetes/pdfs/data/statistics/national-diabetes-statistics-report.pdf

Chang, L., Chiang, S., & Saltiel, A. R. (2010). Insulin signaling and the regulation of glucose transport. *Molecular Medicine, 10*(7-12), 65-71. Retrieved from https://www.ncbi.nlm.nih.gov/pmc/articles/PMC1431367/

Chen, K., Pittman, R. N., & Popel, A. S. (2008a). Nitric oxide in the vasculature: Where does it come from and where does it go? A quantitative perspective. *Antioxidants & Redox Signaling, 10*(7), 1185-1198. doi:10.1089/ars.2007.1959

Chen, K., Pittman, R. N., & Popel, A. S. (2008b). Nitric oxide in the vasculature: Where does it come from and where does it go? A quantitative perspective. *Antioxidants & Redox Signaling, 10*(7), 1185-1198. doi:10.1089/ars.2007.1959

Chestnov, O. (2014). Global status report on noncommunicable diseases. *World Health Organization,* , 9. Retrieved from https://apps.who.int/iris/bitstream/handle/10665/148114/9789241564854_eng.pdf;jsessionid=11DB9EDF6B85966120B1C71D39F4828C?sequence=1

Ciraolo, E., Gulluni, F., & Hirsch, E. (2014). Methods to measure the enzymatic activity of PI3Ks. In L. Galluzzi, & G. Kroemer (Eds.), *Methods in enzymology* (pp. 115-140) Academic Press. Retrieved from http://www.sciencedirect.com/science/article/pii/B9780128013298000064

Cortese-Krott, M. M., Rodriguez-Mateos, A., Kuhnle, G. G. C., Brown, G., Feelisch, M., & Kelm, M. (2012). A multilevel analytical approach for detection and visualization of intracellular NO production and nitrosation events using diaminofluoresceins. *Free Radical Biology and Medicine, 53*, 2146-2158. Retrieved from https://sfrbm.org/site/assets/files/1240/intracellular-no_diaminofluoresceins_kelm_frbm2012.pdf

Creager, M., & Lüscher, T. (2003). Diabetes and vascular disease. *Circulation, 108*(12), 1527-1532. doi:10.1161/01.CIR.0000091257.27563.32

Daiber, A., Steven, S., Weber, A., Shuvaev, V. V., Muzykantov, V. R., Later, I., et al. (2017). Targeting vascular (endothelial) dysfunction. *British Journal of Pharmacology, 174*(12), 1591-1619. Retrieved from https://www.ncbi.nlm.nih.gov/pmc/articles/PMC5446575/

Dangelmaier, C., Manne, B. K., Liverani, E., Jin, J., Bray, P., & Kunapuli, S. P. (2014). PDK1 selectively phosphorylates thr(308) on akt and contributes to human platelet functional responses. *Thrombosis and Haemostasis, 111*(3), 508-517. doi:10.1160/TH13-06-0484

DeFronzo, R. A., & Tripathy, D. (2009). Skeletal muscle insulin resistance is the primary defect in type 2 diabetes.*American Diabetes Association, 32*(2) Retrieved from https://care.diabetesjournals.org/content/32/suppl_2/S157.long

Dhananjayan, R., Koundinya, K. S. S., Malati, T., & Kutala, V. K. (2016). Endothelial dysfunction in type 2 diabetes mellitus. *Indian Journal of Clinical Biochemistry, 31*(4), 372-379. doi:10.1007/s12291-015-0516-y

DiMeglio, L. A., Evans-Molina, C., & Oram, R. A. (2018). Type 1 diabetes. *Lancet, 391*(10138), 2449-2462. Retrieved from https://www.ncbi.nlm.nih.gov/pmc/articles/PMC6661119/

Doege, H., Grimm, D., Falcon, A., Tsang, B., Storm, T. A., Xu, H., et al. (2008). Silencing of hepatic fatty acid transporter protein 5 in vivo reverses diet-induced non-alcoholic fatty liver disease and improves hyperglycemia. *Journal of Biological Chemistry, 283*(32), 22186-22192. Retrieved from https://pubmed.ncbi.nlm.nih.gov/18524776/

Fasshauer, M., Kralisch, S., Klier, M., Lossner, U., Bluher, M., Klein, J., et al. (2003). Adiponectin gene expression and secretion is inhibited by interleukin-6 in 3T3-L1 adipocytes. *Biochemical and Biophysical Research Communications, 301*(4), 1045-1050. Retrieved from https://pubmed.ncbi.nlm.nih.gov/12589818/

Feng, J., Park, J., Cron, P., Hess, D., & Hemmings, B. A. (2004). Identification of a PKB/akt hydrophobic motif ser-473 kinase as DNA-dependent protein kinase. *Journal of Biological Chemistry, 279*(39), 41189-41196. doi:10.1074/jbc.M406731200

Fountain, J. H., & Lappin, S. L. (2020). Physiology, renin angiotensin system. *StatPearls,* Retrieved from https://www.ncbi.nlm.nih.gov/books/NBK470410/

Francis, S. H., Busch, J. L., & Corbin, J. D. (2010). cGMP-dependent protein kinases and cGMP phosphodiesterases in nitric oxide and cGMP action. *Pharmacological Reviews, 62*(3), 525-563. doi:10.1124/pr.110.002907

Freeman, A. M., & Pennings, N. (2020). Insulin resistance. *StatPearls,* Retrieved from https://www.ncbi.nlm.nih.gov/books/NBK507839/

Fujisawa, H., Suma, K., Origuchi, K., Kumagai, H., Seki, T., & Ariga, T. (2008). Biological and chemical stability of garlic-derived allicin. *Journal of Agricultural Food Chemistry, 56*(11), 4229-4235. Retrieved from https://pubmed.ncbi.nlm.nih.gov/18489116/

Funk. Steven Daniel, Yurdagul Jr., A., & Orr, A. W. (2012). Hyperglycemia and endothelial dysfunction in atherosclerosis: Lessons from type 1 diabetes. *International Journal of Vascular Medicine, 2012*, 1-9. Retrieved from https://www.ncbi.nlm.nih.gov/pmc/articles/PMC3303762/

Ghantous, C. M., Azrak, Z., Hanache, S., Abou-Kheir, W., & Zidan, A. (2015). Differential role of leptin and adiponectin in cardiovascular system. *International Journal of Endocrinology, 2015* Retrieved from https://www.hindawi.com/journals/ije/2015/534320/

Ghebremariam, Y. T., Huang, N. F., Kambhampati, S., Volz, K. S., Joshi, G. G., Ansyln, E. V., et al. (2013). Characterization of a fluorescent probe for imaging nitric oxide. *Journal of Vascular Research, 51*(1), 68-79. Retrieved from https://www.ncbi.nlm.nih.gov/pmc/articles/PMC3927988/

Gloria A. Benavides, Giuseppe L. Squadrito, Robert W. Mills, Hetal D. Patel, T. Scott Isbell, Rakesh P. Patel, et al. (2007). Hydrogen sulfide mediates the vasoactivity of garlic. *Proceedings of the National Academy of Sciences - PNAS, 104*(46), 17977-17982. doi:10.1073/pnas.0705710104

Goyal, R., & Jill, I. (2020). Diabetes mellitus type 2. *StatPearls,* Retrieved from https://www.ncbi.nlm.nih.gov/books/NBK513253/

Grillo, A., Salvi, L., Coruzzi, P., Salvi, P., & Parati, G. (2019). Sodium intake and hypertension. *Νθτριεντσ, 11*(9), 1-9. Retrieved from https://www.ncbi.nlm.nih.gov/pmc/articles/PMC6770596/

Han, J., Kim, N., Joo, H., Kim, E., & Earm, Y. E. (2002). ATP-sensitive K+ channel activation by nitric oxide and protein kinase G in rabbit ventricular myocytes. *American Journal of Physiology-Heart and Circulatory Physiology, 283*(4), H1545-H1554. doi:10.1152/ajpheart.01052.2001

Hemmings, B. A., & Restuccia, D. F. (2012). PI3K-PKB/akt pathway. *Cold Spring Harbor Perspectives in Biology, 4*(9), a011189. doi:10.1101/cshperspect.a011189

Holmes, J. W., Nuñez, J. A., & Covell, J. W. (1997). Functional implications of myocardial scar structure. *American Journal of Physiology, 272*(5), H2123-H2130. Retrieved from https://pubmed.ncbi.nlm.nih.gov/9176277/

Horuzsko, D., White, R., & Zhu, S. (2019). Allicin reverses diabetes-induced dysfunction of human coronary artery endothelial cells. *Digital Commons PCOM,* Retrieved from https://digitalcommons.pcom.edu/cgi/viewcontent.cgi?article=1193&context=biomed

Hosoki, R., Matsuki, N., & Kimura, H. (1997). The possible role of hydrogen sulfide as an endogenous smooth muscle relaxant in synergy with nitric oxide. *Biochemical and Biophysical Research Communications, 237*(3), 527-531. doi:10.1006/bbrc.1997.6878

Hubbard, S. R. (2013). The insulin receptor: Both a prototypical and atypical receptor tyrosine kinase. *Cold Spring Harbor Perspectives in Biology, 5*(3) Retrieved from https://www.ncbi.nlm.nih.gov/pmc/articles/PMC3578362/

Inzucchi, S., Bergenstal, R., Fonesca, V., Gregg, E., Mayer-Davis, B., Spollett, H., et al. (2010). Diagnosis and classification of diabetes mellitus. *Diabetes Care, 33*(Suppl 1), S62-S69. doi:10.2337/dc10-S062

Iqbal, A. M., & Jamal, S. F. (2020). Essential hypertension. *StatPearls,* Retrieved from https://www.ncbi.nlm.nih.gov/books/NBK539859/

Jiang, X., Chen, S., Asara, J. M., & Balk, S. P. (2010a). Phosphoinositide 3-kinase pathway activation in phosphate and tensin homolog (PTEN)-deficient prostate cancer cells is independent of receptor tyrosine kinases and mediated by the p110β and p110δ catalytic subunits. *The Journal of Biological Chemistry, 285*(20), 14980-14989. doi:10.1074/jbc.M109.085696

Jiang, X., Chen, S., Asara, J. M., & Balk, S. P. (2010b). Phosphoinositide 3-kinase pathway activation in phosphate and tensin homolog (PTEN)-deficient prostate cancer cells is independent of receptor tyrosine kinases and mediated by the p110β and p110δ catalytic subunits. *The Journal of Biological Chemistry, 285*(20), 14980-14989. doi:10.1074/jbc.M109.085696

Kern, P. A., Saghizadeh, M., Ong, J. M., Bosch, R. J., Deem, R., & Simsolo, R. B. (1995). The expression of tumor necrosis factor in human adipose tissue. regulation by obesity, weight loss, and relationship to lipoprotein lipase.*Journal of Clinical Investigation, 95*(5), 2111-2119. Retrieved from https://pubmed.ncbi.nlm.nih.gov/7738178/

Kobayashi, T., Taguchi, K., Nemoto, S., Naomi, T., Matsumoto, T., & Kamata, K. (2009). Activation of the PDK-1/akt/eNOS pathway involved in aortic endothelial function differs between hyperinsulinemic and insulin-deficient diabetic rats. *American Journal of Physiology, 297*(5), H1767-H1775. Retrieved from https://journals.physiology.org/doi/full/10.1152/ajpheart.00536.2009?rfr_dat=cr_pub++0pubmed&url_ver=Z39.88-2003&rfr_id=ori%3Arid%3Acrossref.org

Kolluru, G. K., Bir, S. C., & Kevil, C. G. (2012). Endothelial dysfunction and diabetes: Effects on angiogenesis, vascular remodeling, and wound healing. *International Journal of Vascular Medicine, 2012*, 1-30. doi:10.1155/2012/918267

Krenz, M., & Robbins, J. (2004). Impact of beta-myosin heavy chain expression on cardiac function during stress.*Journal of the American College of Cardiology, 44*(12), 2390-2397. Retrieved from https://www.sciencedirect.com/science/article/pii/S0735109704019278

Landry, D. W., Anubkumar, S., & Oliver, J. A. (2006). Vascular tone. In R. K. Albert, A. S. Slutsky, V. M. Ranieri, J. Takala & A. Torres (Eds.), *Clinical critical care medicine* (pp. 31-39). Philadelphia: Mosby. Retrieved from http://www.sciencedirect.com/science/article/pii/B9780323028448500093

Lawson, L. D., & Hunsaker, S. M. (2018). Allicin bioavailability and bioequivalence from garlic supplements and garlic foods. *Nutrients, 10*(7) Retrieved from https://www.mdpi.com/2072-6643/10/7/812/htm

Li, H., Wallerath, T., Munzel, T., & Fostermann, U. (2002). Regulation of endothelial-type NO synthase expression in pathophysiology and in response to drugs. *Nitric Oxide, 7*(3), 149-164. Retrieved from https://www.sciencedirect.com/science/article/pii/S1089860302001118?via%3Dihub

Liesivuori, J. (2014). Formic acid. *Encyclopedia of toxicology* (pp. 659-661) Reference Module in Biomedical Sciences.

Lin, F., Yan, Y., Wei, S., Huang, X., Peng, Z., ke, X., et al. (2020). Hydrogen sulfide protects against high glucose-induced human umbilical vein endothelial cell injury through activating PI3K/akt/eNOS pathway. *Drug Design, Development and Theory, 14*, 621-633. Retrieved from https://www.ncbi.nlm.nih.gov/pmc/articles/PMC7027865/

Lin, V. S., Lippert, A. R., & Chang, C. J. (2013). Cell-trappable fluorescent probes for endogenous hydrogen sulfide signaling and imaging H2O2-dependent H2S production. *Pnas, 110*(18), 7131-7135. Retrieved from https://www.ncbi.nlm.nih.gov/pmc/articles/PMC3645565/

Liu, P., Cheng, H., Roberts, T. M., & Zhao, J. J. (2009). Targeting the phosphoinositide 3-kinase (PI3K) pathway in cancer. *Nature Reviews. Drug Discovery, 8*(8), 627-644. doi:10.1038/nrd2926

Lucier, J., & Weinstock, R. S. (2021). Diabetes mellitus type 1. *StatPearls,* Retrieved from https://www.ncbi.nlm.nih.gov/books/NBK507713/

Lusis, A. J. (2000). Atherosclerosis. *Nature, 407*(6801), 233-241. Retrieved from https://www.ncbi.nlm.nih.gov/pmc/articles/PMC2826222/

Ma, L., chen, S., Li, S., Deng, L., Li, Y., & Li, H. (2018). Effect of allicin against ischemia/hypoxia-induced H9c2 myoblast apoptosis via eNOS/NO pathway-mediated antioxidant activity. *Evidence-Based Complementary and Alternative Medicine, 2018* Retrieved from https://www.hindawi.com/journals/ecam/2018/3207973/

Madsen-Rask, C., & King, G. L. (2013). Vascular complications of diabetes: Mechanisms of injury and protective factors. *Cell Metabolism, 17*(1), 20-33. doi:10.1016/j.cmet.2012.11.012

Manna, P., & Jain, S. K. (2011). Hydrogen sulfide and l-cysteine increase phosphatidylinositol 3,4,5-trisphosphate (PIP3) and glucose utilization by inhibiting phosphatase and tensin homolog (PTEN) protein and activating phosphoinositide 3-kinase (PI3K)/serine/threonine protein kinase (AKT)/protein kinase cζ/λ (PKCζ/λ) in 3T3l1 adipocytes. *Journal of Biological Chemistry, 286*(46), 39848-39859. Retrieved from https://www.ncbi.nlm.nih.gov/pmc/articles/PMC3220540/

Martins, A. R., Nachbar, R. T., Gorjao, R., Vinolo, M. A., Festuccia, W. T., Lambertucci, R. H., et al. (2012). Mechanisms underlying skeletal muscle insulin resistance induced by fatty acids: Importance of the mitochondrial function.*Lipids in Health and Disease, 11*(30) Retrieved from https://lipidworld.biomedcentral.com/articles/10.1186/1476-511X-11-30#citeas

Matsubara, M., Maruoka, S., & Katayose, S. (2002). Decreased plasma adiponectin concentrations in women with dyslipidemia. *Journal of Clinical Endocrinology Metabolism, 87*(6), 2764-2769. Retrieved from https://pubmed.ncbi.nlm.nih.gov/12050247/

Mendis, S., Puska, P., & Norrving, B. (2014). Global atlas on cardiovascular disease prevention and control. *World Health Organization in Collaboration with the World Heart Foundation and the World Stroke Foundation,* , 2-4. Retrieved from https://web.archive.org/web/20140817123106/http://whqlibdoc.who.int/publications/2011/9789241564373_eng.pdf?ua=1

Miao, B., Skidan, I., Yang, J., Lugovskoy, A., Reibarkh, M., Long, K., et al. (2010). Small molecule inhibition of phosphatidylinositol-3,4,5-triphosphate (PIP3) binding to pleckstrin homology domains. *Proceedings of the National Academy of Sciences, 107*(46), 20126-20131. Retrieved from https://www.pnas.org/content/107/46/20126

Michell, B. J., Griffiths, J. E., Mitchelhill, K. I., Rodriguez-Crespo, I., Tiganis, T., Bozinovski, S., et al. (1999). The akt kinase signals directly to endothelial nitric oxide synthase. *Current Biology: CB, 9*(15), 845-848. doi:10.1016/s0960-9822(99)80371-6

Minokoshi, Y., Kim, Y., Peroni, O. D., Fryer, L. G. D., Muller, C., Carling, D., et al. (2002). Leptin stimulates fatty-acid oxidation by activating AMP-activated protein kinase. *Nature, 415*(6869), 339-343. Retrieved from https://pubmed.ncbi.nlm.nih.gov/11797013/

Molgaard, S., Ulrichsen, M., Olsen, D., & Glerup, S. (2016). Detection of phosphorylated akt and MAPK in cell culture assays. *MethodsX, 3*, 386-398. doi:10.1016/j.mex.2016.04.009

Montfort, W. R., Wales, J. A., & Weichsel, A. (2017). Structure and activation of soluble guanylyl cyclase, the nitric oxide sensor. *Antioxidants & Redox Signaling, 26*(3), 107-121. doi:10.1089/ars.2016.6693

Muoio, D. M., & Newgard, C. B. (2008). Molecular and metabolic mechanisms of insulin resistance and β-cell failure in type 2 diabetes. *Nature Reviews, 9*, 193-205. Retrieved from https://www.nature.com/articles/nrm2327

Musicki, B., & Burnett, A. L. (2006). Endothelial dysfunction in diabetic erectile dysfunction. *International Journal of Impotence Research, 19*, 129-138. Retrieved from https://www.nature.com/articles/3901494.pdf?origin=ppub

New, D. C., Wu, K., Kwok, A. W. S., & Wong, Y. H. (2007). G protein-coupled receptor-induced akt activity in cellular proliferation and apoptosis. *The FEBS Journal, 274*(23), 6025-6036. doi:10.1111/j.1742-4658.2007.06116.x

Nicholson, K. M., & Anderson, N. G. (2002). The protein kinase B/akt signalling pathway in human malignancy. *Cellular Signalling, 14*(5), 381-395. doi:10.1016/S0898-6568(01)00271-6

Novack, M. L., & Zevitz, M. E. (2021). Natriuretic peptide B type test. *StatPearls,* Retrieved from https://www.ncbi.nlm.nih.gov/books/NBK556136/

Ogobuiro, I., Wehrle, C. J., & Tuma, F. (2020). Anatomy, thorax, heart coronary arteries. *StatPearls* (). Treasure Island (FL): StatPearls Publishing. Retrieved from http://www.ncbi.nlm.nih.gov/books/NBK534790/

Ojha, N., Dhamoon, & Amit, S. (2020). Myocardial infarction . *StatPearls,* Retrieved from https://www.ncbi.nlm.nih.gov/books/NBK537076/

Oparil, S., Acelakado, M. C., Bakris, G. L., Berlowitz, D. R., Cifkova, R., Dominiczak, A. F., et al. (2018). Hypertension. *National Reviews Disease Primers, 4*(18014), 2-10. Retrieved from https://www.ncbi.nlm.nih.gov/pmc/articles/PMC6477925/

Oral, E. O., Simha, V., Ruiz, E., Andwelt, A., Premkumar, A., Snell, P., et al. (2002). Leptin-replacement therapy for lipodystrophy. *The New England Journal of Medicine, 346*, 570-578. Retrieved from https://www.nejm.org/doi/full/10.1056/nejmoa012437

Osaki, M., Oshimura, M., & Ito, H. (2004). PI3K-akt pathway: Its functions and alterations in human cancer. *Apoptosis, 9*, 667-676. Retrieved from https://link.springer.com/article/10.1023/B:APPT.0000045801.15585.dd

Oyama, Y., Sakai, H., Arata, T., Okano, Y., Akaike, N., Sakai, K., et al. (2002). Cytotoxic effects of methanol, formaldehyde, and formate on dissociated rat thymocytes: A possibility of aspartame toxicity. *Cell Biology and Toxicology, 2002*(18), 43-50. Retrieved from https://link.springer.com/content/pdf/10.1023/A:1014419229301.pdf

Pan, J., Yuan, H., Zhang, X., Zhang, H., Xu, Q., Zhou, Y., et al. (2017). Probing the molecular mechanism of human soluble guanylate cyclase activation by NO in vitro and in vivo. *Scientific Reports, 7*(1), 43112. doi:10.1038/srep43112

Paneni, F., Beckman, J. A., Creager, M. A., & Cosentino, F. (2013). Diabetes and vascular disease: Pathophysiology, clinical consequences, and medical therapy: Part I. *European Heart Journal, 34*(31), 2436-2443. Retrieved from https://www.ncbi.nlm.nih.gov/pmc/articles/PMC3743069/

Paschou, S. A., Papadopoulou-Marketou, N., Chrousos, G. P., & Kanaka-Gantenbein, C. (2017). On type 1 diabetes mellitus pathogenesis. *Endocrine Connections, 7*(1), R38-R46. Retrieved from https://www.ncbi.nlm.nih.gov/pmc/articles/PMC5776665/

Pasmanter, N., Iheanacho, F., & Hashmi, M. F. (2020). Biochemistry, cyclic GMP. *StatPearls* (). Treasure Island (FL): StatPearls Publishing. Retrieved from http://www.ncbi.nlm.nih.gov/books/NBK542234/

Perry, R. J., Samuel, V. T., Petersen, K. F., & Shulman, G. I. (2014). The role of hepatic lipids in hepatic insulin resistance and type 2 diabetes. *Nature, 510*(7503), 84-91. Retrieved from https://www.ncbi.nlm.nih.gov/pmc/articles/PMC4489847/

Petersen, M. c., & Shulman, G. I. (2018). Mechanisms of insulin action and insulin resistance. *Physiological Reviews, 98*(4), 2133-2223. Retrieved from https://www.ncbi.nlm.nih.gov/pmc/articles/PMC6170977/

Peterson, M. c., & Shulman, G. I. (2018). Mechanisms of insulin action and insulin resistance. *Physiological Reviews, 98*(4), 2133-2223. Retrieved from https://www.ncbi.nlm.nih.gov/pmc/articles/PMC6170977/

Pittas, A. G., Joseph, N. A., & Greenberg, A. S. (2004). Adipocytokines and insulin resistance. *The Journal of Clinical Endocrinology & Metabolism, 89*(2), 447-452. Retrieved from https://academic.oup.com/jcem/article/89/2/447/2840733

Predmore, B. L., Julian, D., & Cardounel, A. J. (2011). Hydrogen sulfide increases nitric oxide production from endothelial cells by an akt-dependent mechanism. *Frontiers in Physiology, 2*, 104. doi:10.3389/fphys.2011.00104

Qin, Y., Dey, A., & Daaka, Y. (2013). Chapter nineteen - protein S-nitrosylation measurement. In M. Conn (Ed.), *Methods in enzymology* (pp. 409-425) Elsevier.

Rafikov, R., Fonseca, F. V., Kumar, S., Pardo, D., Darragh, C., Elms, S., et al. (2011a). eNOS activation and NO function: Structural motifs responsible for the posttranslational control of endothelial nitric oxide synthase activity. *The Journal of Endocrinology, 210*(3), 271-284. doi:10.1530/JOE-11-0083

Rafikov, R., Fonseca, F. V., Kumar, S., Pardo, D., Darragh, C., Elms, S., et al. (2011b). eNOS activation and NO function: Structural motifs responsible for the posttranslational control of endothelial nitric oxide synthase activity. *Journal of Endocrinology, 210*(3), 271-284. Retrieved from https://www.ncbi.nlm.nih.gov/pmc/articles/PMC3326601/

Rajala, M. W., Obici, S., Scherer, P. E., & Rossetti, L. (2003). Adipose-derived resistin and gut-derived resistin-like molecule-beta selectively impair insulin action on glucose production. *Journal of Clinical Investigation, 111*(2), 225-230. Retrieved from https://pubmed.ncbi.nlm.nih.gov/12531878/

Randle, P. J., Garland, P. B., Hales, C. N., & Newsholme, E. A. (1963). The glucose fatty-acid cycle. its role in insulin sensitivity and the metabolic disturbances of diabetes mellitus. *Lancet, 1*(7285), 785-789. Retrieved from https://pubmed.ncbi.nlm.nih.gov/13990765/

Roden, M., Price, T. B., Perseghin, G., Petersen, K. F., Rothman, D. L., Cline, G. W., et al. (1996). Mechanism of free fatty acid-induced insulin resistance in humans. *The Journal of Clinical Investigation, 97*(12), 2859-2865. Retrieved from https://pubmed.ncbi.nlm.nih.gov/8675698/

Sarbassov, D. D., Guertin, D. A., Ali, S. M., & Sabatini, D. M. (2005). Phosphorylation and regulation of akt/PKB by the rictor-mTOR complex. *Science, 307*(5712), 1098-1101. Retrieved

from https://science.sciencemag.org/content/307/5712/1098.abstract?ijkey=776975788499e7d50835c058c479fe9df4eaa113&keytype2=tf_ipsecsha

Saxton, A., Chaudhry, R., & Manna, B. (2020). Anatomy, thorax, heart right coronary arteries. *StatPearls* (). Treasure Island (FL): StatPearls Publishing. Retrieved from http://www.ncbi.nlm.nih.gov/books/NBK537357/

Scott, J. (2004). Pathophysiology and biochemistry of cardiovascular disease. *Current Opinion in Genetics & Development, 14*(3), 271-279. Retrieved from https://www.sciencedirect.com/science/article/pii/S0959437X04000589?via%3Dihub

Sessa, W. C. (2014). eNOS at a glance. *Journal of Cell Science, 117*, 2427-2429. Retrieved from https://jcs.biologists.org/content/117/12/2427

Shahjehan, R. D., & Bhutta, B. S. (2021). Coronary artery disease. *StatPearls,* Retrieved from https://www.ncbi.nlm.nih.gov/books/NBK564304/

Shi, X., Wang, J., Lei, Y., Cong, C., Tan, D., & Zhou, X. (2019). Research progress on the PI3K/AKT signaling pathway in gynecological cancer (review). *Molecular Medicine Reports, 19*(6), 4529-4535. doi:10.3892/mmr.2019.10121

Sigma-Aldrich. (2013). Hydrogen sulfide test strips. Retrieved from https://www.sigmaaldrich.com/content/dam/sigma-aldrich/docs/Sigma-Aldrich/Datasheet/1/06728dat.pdf

Song, C., Liu, B., Shi, Y., Liu, N., Yan, Y., Zhang, J., et al. (2016). MicroRNA-130a alleviates human coronary artery endothelial cell injury and inflammatory responses by targeting PTEN via activating PI3K/akt/eNOS signaling pathway. *Oncotarget, 7*(44), 71922-71936. doi:10.18632/oncotarget.12431

Steensberg, A., Fischer, C. P., Sacchetti, M., Keller, c., Osada, T., Schjerling, P., et al. (2003). Acute interleukin-6 administration does not impair muscle glucose uptake or whole-body glucose disposal in healthy humans. *The Journal of Physiology, 548*(2), 631-638. Retrieved from https://pubmed.ncbi.nlm.nih.gov/12640021/

Szendroedi, J., Yoshimura, T., Philip, E., Kolaiki, C., Marcus, M., Zhang, D., et al. (2014). Role of diacylglycerol activation of PKCθ in lipid-induced muscle insulin resistance in humans. *Pnas, 111*(26), 9597-9602. Retrieved from https://pubmed.ncbi.nlm.nih.gov/24979806/

Takahashi, T., & Harris, R. C. (2014). Role of endothelial nitric oxide synthase in diabetic nephropathy: Lessons from diabetic eNOS knockout mice. *Journal of Diabetes Research, 2014* Retrieved from https://www.hindawi.com/journals/jdr/2014/590541/

Takimoto, E., & Kass, D. A. (2012). Regulation of cardiac systolic function and contractility. In J. A. Hill, & E. N. Olson (Eds.), *Muscle* (pp. 285-297). Boston/Waltham: Academic Press. Retrieved from http://www.sciencedirect.com/science/article/pii/B9780123815101000211

Unger, R. H., Zhou, Y. T., & Orci, L. (1999). Regulation of fatty acid homeostasis in cells: Novel role of leptin. *Pnas, 96*(5), 2327-2332. Retrieved from https://pubmed.ncbi.nlm.nih.gov/10051641/

Vargas, E., Joy, N. V., & Sepulveda, M. A. C. (2021). Biochemistry, insulin metabolic effects. *StatPearls,* Retrieved from https://www.ncbi.nlm.nih.gov/books/NBK525983/

Vargas, E., Podder, V., & Sepulveda, M. A. C. (2020). Physiology, glucose transporter type 4. *StatPearls,* Retrieved from https://www.ncbi.nlm.nih.gov/books/NBK537322/

Villa, A. D., Sammut, E., Nair, A., Rajani, R., Bonamini, R., & Chiribiri, A. (2016). Coronary artery anomalies overview: The normal and the abnormal. *World Journal of Radiology, 8*(6), 537-555. doi:10.4329/wjr.v8.i6.537

Wallenius, V., Wallenius, K., Ahren, B., Rudling, M., Carlsten, H., Dickson, S. L., et al. (2002). Interleukin-6-deficient mice develop mature-onset obesity. *Nature Medical, 8*(1), 75-79. Retrieved from https://pubmed.ncbi.nlm.nih.gov/11786910/

Wang, T., Wang, J., Hu, X., Huang, X., & Chen, G. (2020). Current understanding of glucose transporter 4 expression and functional mechanisms. *World Journal of Biological Chemistry, 11*(3), 76-98. Retrieved from https://www.ncbi.nlm.nih.gov/pmc/articles/PMC7672939/

Wang, W., Wang, D., Kong, C., Li, S., Xie, L., Lin, Z., et al. (2019). eNOS S-nitrosylation mediated OxLDL-induced endothelial dysfunction via increasing the interaction of eNOS with β-catenin. *Biochimica Et Biophysica Acta (BBA) - Molecular Basis of Disease, 1865*(7), 1793-1801. Retrieved from https://www.sciencedirect.com/science/article/pii/S0925443918300668

Weyer, C., Funahashi, T., Tanaka, S., Hotta, K., Matsuzawa, Y., Partly, R. E., et al. (2001). Hypoadiponectinemia in obesity and type 2 diabetes: Close association with insulin resistance and hyperinsulinemia. *Journal of Clinical Endocrinology Metabolism, 86*(5), 1930-1935. Retrieved from https://pubmed.ncbi.nlm.nih.gov/11344187/

Wilcox, G. (2005). Insulin and insulin resistance. *The Clinical Biochemist Reviews, 26*(2), 19-39. Retrieved from https://www.ncbi.nlm.nih.gov/pmc/articles/PMC1204764/

Yamauchi, T., Kamon, J., Waki, H., Terauchi, Y., Kubota, N., Hara, K., et al. (2001). The fat-derived hormone adiponectin reverses insulin resistance associated with both lipoatrophy and obesity. *Nature Medicine, 7*(8), 941-946. Retrieved from https://pubmed.ncbi.nlm.nih.gov/11479627/

Yu, S. B., & Pekkurnaz, G. (2018). Mechanisms orchestrating mitochondrial dynamics for energy homeostasis. *Journal of Molecular Biology, 430*(21), 3922-3941. Retrieved from https://pubmed.ncbi.nlm.nih.gov/30089235/

Yu, S., Wong, S. L., Lau, C. W., Huang, Y., & Yu, C. (1959). Biochemical and biophysical research communications. *Biochemical and Biophysical Research Communications, 407*(1), 44-48. Retrieved from http://www.sciencedirect.com/science/article/pii/S0006291X11003019

Yu, X., Fu, Y., Zhang, D., Yin, K., & Tang, C. (2013). Foam cells in atherosclerosis. *Clinica Chimica Acta, 424*, 245-252. Retrieved from https://www.sciencedirect.com/science/article/pii/S0009898113002477?via%3Dihub

Zhang, C., Zhou, B., Sheng, J., Chen, Y., Cao, Y., & Chen, C. (2020). Molecular mechanisms of hepatic insulin resistance in nonalcoholic fatty liver disease and potential treatment

strategies. *Pharmacological Research, 159* Retrieved from https://www.sciencedirect.com/science/article/pii/S1043661820312925

Zhang, X., Shai, H., & Zheng, X. (2019). Amino acids at the intersection of nutrition and insulin sensitivity . *Drug Discovery Today, 24*(4), 1038-1043. Retrieved from https://www.sciencedirect.com/science/article/pii/S1359644618303799?via%3Dihub

Zhang, Y., Proenca, R., Maffei, M., Barone, M., Leopold, L., & Friedman, J. M. (1994). Positional cloning of the mouse obese gene and its human homologue. *Nature, 372*(6505), 425-432. Retrieved from https://pubmed.ncbi.nlm.nih.gov/7984236/

Zhang, Y., Proence, R., Maffel, M., Baron, M., Leopold, L., & Friedman, J. M. (1994). Positional cloning of the mouse *obese* gene and its human homologue. *Nature, 372*, 425-431. Retrieved from https://www.nature.com/articles/372425a0.pdf

Zhao, Y., Vanhoutte, P. M., & Leung, S. W. S. (2015). Vascular nitric oxide: Beyond eNOS. *Journal of Pharmacological Sciences, 129*(2), 83-94. doi:10.1016/j.jphs.2015.09.002